MICROCOPY RESOLUTION TEST CHART

NATIONAL BUREAU OF STANDARDS - 1963 - A

BR99572.

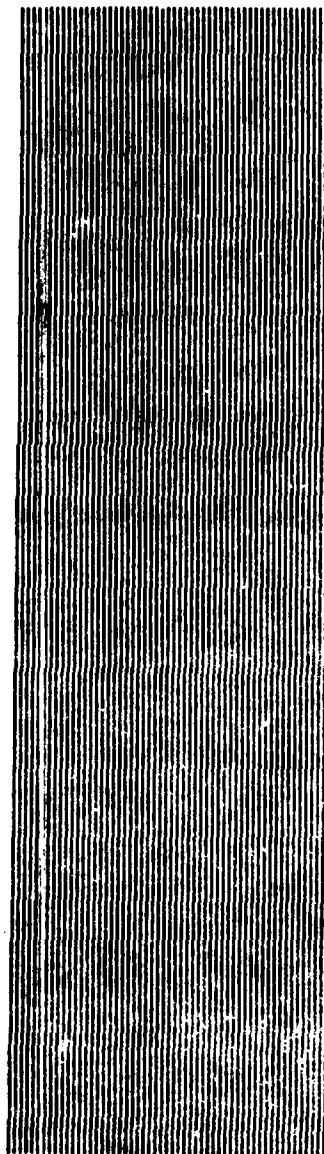Report No. 85016

ROYAL SIGNALS AND RADAR ESTABLISHMENT,
MALVERN

AD-A169 895

AN INTRODUCTION TO RADAR ABSORBENT
MATERIALS (RAM)

Author: P G Lederer

DTIC
ELECTE
JUL 2 1 1986

E

PROCUREMENT EXECUTIVE, MINISTRY OF DEFENCE
RSRE
Malvern, Worcestershire.

86 7 15 103 February 1986

ROYAL SIGNALS AND RADAR ESTABLISHMENT

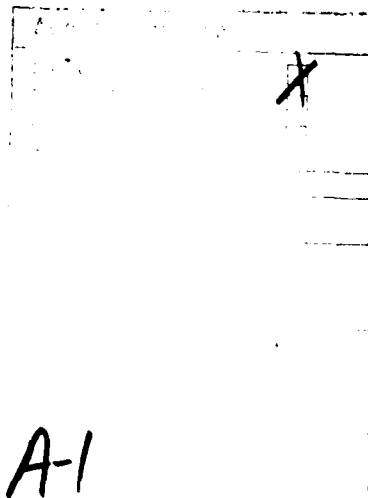**Report No** 85016

TITLE: AN INTRODUCTION TO RADAR ABSORBENT
MATERIALS (RAM)

AUTHOR: P G Lederer

DATE: February 1986

SUMMARY

The purpose of this Introduction is to present, in a straightforward
way, the electromagnetic principles of Radar Absorbent Materials (RAM)
for the benefit of the non-electromagnetic-specialist who finds himself
involved in this field. The fundamental theory of electromagnetic wave
propagation in media and at the interfaces between different media is
reviewed and the various approaches to absorber design are described in
the light of this. The types of materials required and the techniques
for measuring both their electromagnetic properties and the performance
of the finished abosrber are outlined. Finally a means of designing
absorbers from a knowledge of the properties of its constituent materials
is described.

A-1

CONTENTS

1. INTRODUCTION

2. ELECTROMAGNETIC FUNDAMENTALS

   2.1 Material Properties
   2.2 Reflection and Refraction at Boundaries and Impedance Matching
   2.3 Finite Layers

3. ABSORBER TYPES

   3.1 General Requirements
   3.2 Pyramidal Absorbers
   3.3 Tapered Loading
   3.4 Matching Layer
   3.5 Tuned Layer
   3.6 Salisbury Screen
   3.7 Techniques for Improving Bandwidth

4. MATERIALS FOR RAM

   4.1 Composite RAM
   4.2 Binder Materials
   4.3 Lossy Fillers
   4.4 Ferrites

5. MEASUREMENTS

   5.1 Reflectivity Measurement
   5.2 Material Constant Measurement
   5.3 Transmission Line Methods
   5.4 Time Domain Methods

6. ABSORBER DESIGN

   6.1 Transmission Line Model
   6.2 Matrix Elements
   6.3 Oblique Incidence
   6.4 Design of Absorbers

7. REFERENCES

APPENDICES: A.1 Effective Impedance of Multilayer Structures
             A.2 Propagation and Wavelength in Lossy Media
             A.3 Dielectric Slab Sandwiched Between Two Media
             A.4 The Decibel (dB) for Expressing Reflectivity

1. INTRODUCTION

There are many circumstances in which it is necessary to control the reflection of microwave radiation from surfaces. For example, in order that a microwave anechoic chamber may fulfil its purpose of simulating free space in a confined volume, its walls must be rendered non-reflecting by lining them with an electromagnetically absorbent material. The severely limited performance of many surveillance radar systems, particularly those at sea, due to very strong return signals from nearby objects such as masts, buildings or bridges may be improved by coating these objects with an absorbent layer. A similar approach is being used to solve the problem of television 'ghost images' in Japanese cities due to multiple reflections of the broadcast signal by nearby buildings. Nor has the potential contribution of microwave absorbing materials to the reduction in the detectability of targets by radars escaped the notice of the military planners, as recent press reports on the American 'Stealth' programme bear witness.

The electromagnetic demands placed on radar absorbent materials, or RAM, as it usually called, vary according to the specific application, and there is no panacea capable of universal use. The lining of an anechoic chamber, for example, must provide very high levels of energy absorption over a wide frequency range whereas radar obstructions and television ghost images require treatment only at a single frequency. In the military field, wideband coverage is generally required but environmental conditions and restrictions on size and weight are much more severe. The design of absorbers, therefore, must be tailored to each application, and this requires an understanding of the factors which can influence performance. Most absorbers rely on the bulk electromagnetic properties of materials, but, at microwave frequencies, the wavelength of the radiation is of the same order as the dimensions of absorbing structures (a few mm to a few cm) and, consequently, geometrical factors also play an important role.

1

A practical electromagnetic absorber must satisfy two main requirements - it must reduce the reflection of incident radiation by the specified degree over the frequency band of interest and it must achieve this - and continue to achieve it throughout its life - in its operational environment.

Environmental conditions may range from the benignity of an anechoic chamber to the ferocity of the external surfaces of a supersonic jet aircraft, while mechanical constraints may demand anything from a simple self-supporting layer to a full load-bearing member. It is, therefore, clear that this is a cross-disciplinary field calling on expertise both in the structural and chemical integrity of materials and in their electromagnetic properties. Unfortunately these are very diverse disciplines so that the majority of chemists and materials technologists have little or no background in electro-magnetics and vice versa. The problem, therefore, tends to divide naturally into its technological and electrical aspects, but a successful design must involve a collaboration between the two. The purpose of this Introduction is to help to improve the communication process by presenting the electromagnetic aspects of microwave absorbers in a straightforward manner for the benefit of the materials technologist.

The emphasis is on principles rather than a full and detailed treatment, but references are provided to point the way towards deeper study. Firstly, the electromagnetic fundamentals are briefly reviewed; a fuller explanation being given in any one of a number of standard text books of which (1a) is particularly recommended as it has been written very much from a materials point of view. In chapter 3, the various types of absorber are explained in terms of these ideas, and the types of material that exhibit the desired properties are discussed in chapter 4. Chapter 5 reviews the techniques available for measuring both the reflectivity of absorbers and the electro-magnetic parameters of materials. Finally, in chapter 6, the topics of previous chapters are tied together in considering the electromagnetic design of absorbers.

2. ELECTROMAGNETIC FUNDAMENTALS

2.1 Material Properties

In general, the electric and magnetic properties of a dielectric material are characterised by the complex permittivity, ε^*, and the complex permeability, μ^*:

$$\varepsilon^* = \varepsilon' - j\varepsilon'' \quad , \quad \mu^* = \mu' - j\mu'' \quad\quad (2.1)$$

or more frequently, by the relative permittivity, ε_r^*, and relative permeability, μ_r^*:

$$\varepsilon_r^* = \frac{\varepsilon^*}{\varepsilon_o} = \varepsilon_r' - j\varepsilon_r'' \quad , \quad \mu_r^* = \frac{\mu^*}{\mu_o} = \mu_r' - j\mu_r'' \quad . \quad (2.2)$$

The universal constants, ε_o and μ_o, are respectively the permittivity and permeability of free space and are related by

$$\varepsilon_o \mu_o = 1/c^2$$

where c is the velocity of electromagnetic propagation in free space and μ_o is defined as $4\pi \times 10^{-7}$ H m^{-1}.

The real part of the permittivity (or permeability) is a measure of the extent to which the material will be polarised (or magnetised) by the application of an electric (or magnetic) field. The imaginary part is a measure of the energy losses incurred in re-arranging the alignment of the electric (or magnetic) dipoles in that applied field. If an ac electric field is applied across a dielectric slab (as in a capacitor), an ac "displacement" current is observed which is due to the oscillation of the electric dipoles with the field. The dielectric, therefore, possesses an ac conductivity, which is quite independent of any dc conductivity (due to the migration of free charge carriers) that may also exist. The relationship between the total conductivity (ac + dc), σ, and the dielectric loss is[1]

$$\epsilon'' = \frac{\sigma}{\omega} \qquad (2.3)$$

where ω is the angular frequency of the applied field.

If a plane electromagnetic wave, of angular frequency, ω, is propagating in the x-direction through such a dielectric material, the electric and magnetic field vectors, which are normal to each other and to the direction of propagation, are given as functions of time and space, by:

$$\underline{E} = E_o \exp(j\omega t - \gamma x)$$

$$\qquad (2.4)$$

$$\underline{H} = H_o \exp(j\omega t - \gamma x)$$

where γ is the complex propagation factor,

$$\gamma = \alpha + j\beta = j\omega(\epsilon^*\mu^*)^{\frac{1}{2}} \qquad (2.5)$$

The real and imaginary parts of γ define the way in which the amplitude and phase respectively of the wave vary with distance of propagation, α being called the attenuation factor and β the phase factor, given by

$$\beta = \frac{2\pi}{\lambda} \qquad . \qquad (2.6)$$

It is possible to define, in direct analogy to Ohm's Law, a wave impedance, as the ratio of the electric to magnetic fields, and since the E and H components of the wave are uniquely related to each other, this impedance, the intrinsic impedance, Z, is dependent upon the electromagnetic material constants, and is therefore a characteristic of the material:

$$Z = \frac{\underline{E}}{\underline{H}} = \left(\frac{\mu^*}{\epsilon^*}\right)^{\frac{1}{2}} \qquad (2.7)$$

The normalised intrinsic impedance, relative to the intrinsic impedance of free space, Z_o, where

4

$$Z_o = \left(\frac{\mu_o}{\varepsilon_o}\right)^{\frac{1}{2}}$$

is therefore

$$\frac{Z}{Z_o} = \left(\frac{\mu_r^*}{\varepsilon_r^*}\right)^{\frac{1}{2}} \tag{2.8}$$

2.2 Reflection and Refraction at Boundaries and Impedance Matching

When a plane electromagnetic wave is propagating through medium 1 and is incident upon a second medium, medium 2, as shown in Figure 2.1, part of the energy is reflected at the interface and part is transmitted (refracted), the process being completely described by Snell's and Fresnel's Laws. If the incident electric and magnetic fields are E_i and H_i respectively, then the reflected components will be E_r and H_r and the transmitted components E_t and H_t. These are related by

$$E_i + E_r = E_t \qquad \text{(a)}$$
$$\tag{2.9}$$
$$H_i + H_r = H_t \qquad \text{(b)}$$

However, since electric and magnetic fields are related by the intrinsic impedances of the medium according to equation (2.7), it follows that

$$\frac{E_i}{Z_1} - \frac{E_r}{Z_1} = \frac{E_t}{Z_2} \qquad . \qquad \text{(c)} \tag{2.9}$$

The negative sign associated with the reflected component arises as a result of the reversal of the direction of propagation. If the electric field reflection coefficient, Γ, is defined by

$$\Gamma \equiv \frac{E_r}{E_i} \qquad , \tag{2.10}$$

5

MEDIUM 1 Z_1

MEDIUM 2 Z_2

E_i INCIDENT

REFRACTED $(1-\Gamma).E_i = E_t$

$E_r = \Gamma.E_i$ REFLECTED
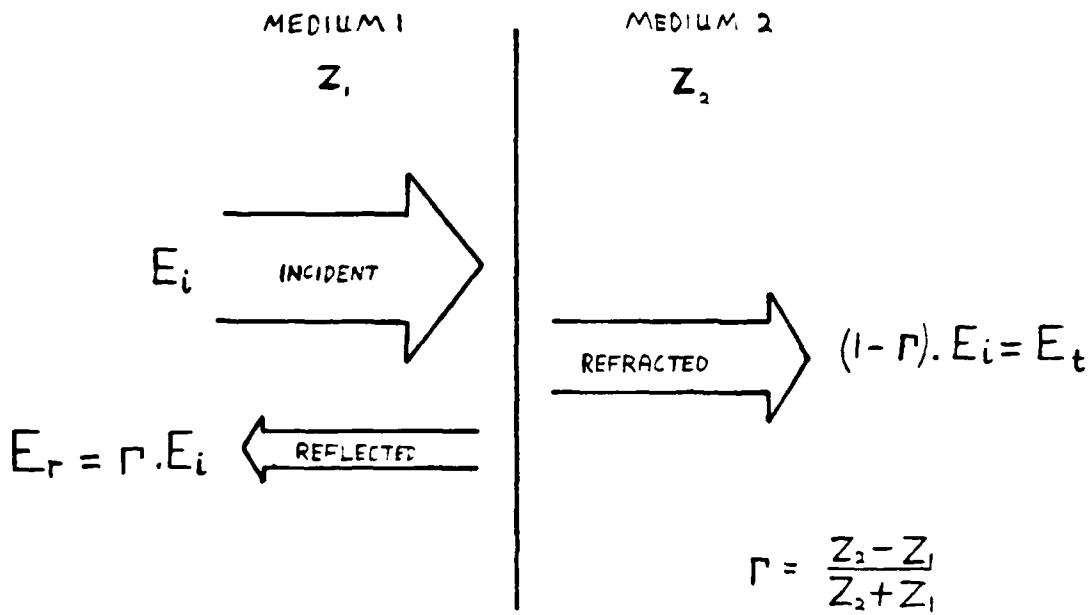
$$\Gamma = \frac{Z_2 - Z_1}{Z_2 + Z_1}$$

Fig. 2.1   Reflection and refraction of incident electromagnetic wave at the boundary between two media

MEDIUM 1   MEDIUM 2   MEDIUM 3   MEDIUM 4
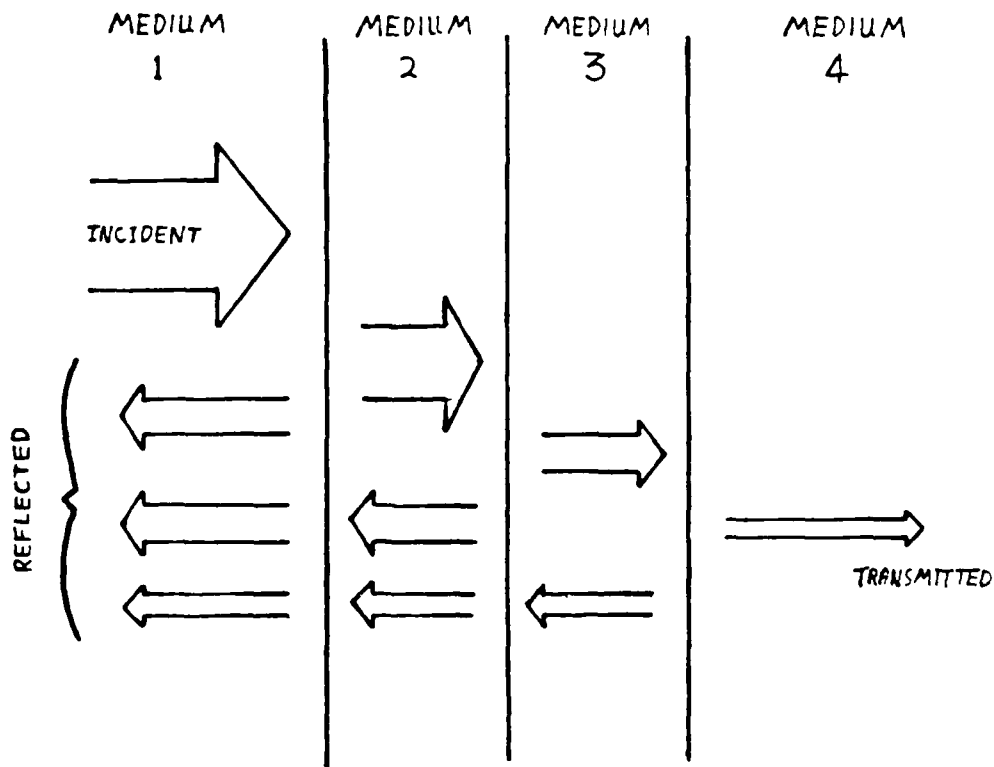
INCIDENT

REFLECTED

TRANSMITTED

Fig. 2.2   Reflection from the various medium boundaries in a multilayer structure

then it follows from equations (2.9a) and (2.9c) that

$$\Gamma = \frac{Z_2 - Z_1}{Z_2 + Z_1} \qquad . \qquad (2.11a)$$

Thus, the reflection coefficient depends only on the intrinsic impedances of the two media and hence on their dielectric and magnetic properties. If, furthermore, medium 1 is air (which, to a very good approximation can be regarded as free space), then equation (2.11a) reduces to

$$\Gamma = \frac{\dfrac{Z_2}{Z_0} - 1}{\dfrac{Z_2}{Z_0} + 1} \qquad (2.11b)$$

where Z_0 is the intrinsic impedance of free space, and Z_2/Z_0 is the normalised intrinsic impedance of medium 2.

Metals have very high values of electrical conductivity and, by equation (2.3), consequently have high values of ε_r'' (at least, at sub-optical frequencies). According to equation (2.7), this confers on them very small values of wave impedance, Z, which leads (by equation (2.11)) to values of reflection coefficient very close to −1. Thus, metals act as almost perfect reflectors of incident electromagnetic radiation (with a phase change of π in the electric field). Similarly, a non-conducting dielectric with a very high value of ε_r' will also have a small wave impedance and a reflection coefficient close to −1. In both of these cases, the impedance of medium 2 is poorly matched to the impedance of medium 1 (free space in the cases considered here) and a high reflection coefficient results. If, however, medium 2 is a material for which

$$\frac{\mu_2^*}{\varepsilon_2^*} = \frac{\mu_1^*}{\varepsilon_1^*} \qquad ,$$

6

then the impedances of the two media are equal, $(Z_2 = Z_1)$ and, according to equation (2.9), the reflection coefficient falls to zero – this condition is referred to as a perfect impedance match. If medium 1 is free space, then the matching condition requires that $\mu_2^* = \epsilon_2^*$, which implies that both real and imaginary parts are equal.

2.3 Finite Layers

The preceding discussion has been restricted to a pair of semi-infinite media, where a reflection was found to occur at the boundary between the two, and the reflection coefficient was found to depend only on the material properties of each. If medium 2, however, has a finite thickness beyond which lies medium 3, (and possibly media 4, 5 etc beyond that) then additional reflections will occur at these subsequent interfaces which will contribute to the total reflected wave seen in medium 1 (Figure 2.2). The total reflected wave, therefore, depends, not only on the nature of medium 2, but also on the materials comprising the subsequent layers and the layer thicknesses. The incident wave sees an effective impedance, Z_L, at the first boundary, which is no longer simply Z_2 but is modified by some function of d_2, Z_3, d_3, Z_4, d_4 etc:

$$Z_L = Z_2 \cdot Fn(d_2, Z_3, d_3, \text{ etc})$$

where Z_i and d_i are the intrinsic impedance and thickness respectively of the ith layer. Having thus defined Z_L, the reflection coefficient of the system of dielectric layers is given by a similar equation

$$\Gamma = \frac{Z_L - Z_1}{Z_L + Z_1} \qquad (2.11c)$$

and the concept of impedance matching is still valid – but now there are more parameters that can be varied in order to achieve it.

It is shown in Appendix A1 that Z_L can be expressed in terms of the impedance and propagation factor of layer 2, Z_2 and γ_2, the thickness of layer 2, d_2, and the effective input impedance of the combination of all

the subsequent layers, Z_T (see Figure A1.1):

$$Z_L = \frac{Z_2 Z_T + Z_2 \tanh \gamma_2 d_2}{Z_2 + Z_T \tanh \gamma_2 d_2} \qquad (2.12)$$

Z_T can also be expressed by a similar expression involving Z_3, γ_3, d_3 and Z_T' (the effective impedance of the 4th and subsequent layers), and this process can be repeated indefinitely. It is apparent that the analysis of a multilayer structure is very complicated, but it is possible to consider some simple cases without difficulty. Two cases of particular importance are the short and open circuit terminations, shown in Figure 2.3. If the layer is intimately backed by a metal, ie a short circuit, then $Z_T = 0$ and 2.12 reduces to

$$Z_L = Z_2 \tanh \gamma_2 d_2 \qquad . \qquad (2.13)$$

If Z_T is infinite, ie an open circuit, (2.12) reduces to

$$Z_L = Z_2 \coth \gamma_2 d_2 \qquad . \qquad (2.14)$$

In order to physically realise this condition $Z_T = \infty$, a short circuit (metal plate) is positioned behind the layer of medium 2 by a distance equal to 1/4 of the wavelength as shown in Figure 2.3. If we consider this 1/4-wavelength spacer in isolation, it is apparent that it can be treated as a special case of the short circuit termination. Equation (2.13), therefore, applies with (assuming the medium to be air) $Z_L = Z_T$, $Z_2 = Z_0$, $d_2 = \lambda_0/4$ and $\gamma_2 = j\beta_0 = j2\pi/\lambda_0$. The tanh function reduces to $j\tan\pi/2$, confirming that the effective impedance of this configuration is infinite. Note, however, that for this to occur, it is necessary for γ_2 to become purely imaginary, which requires that the medium of the spacer is lossless.

A third case, in which the termination consists of another semi-infinite layer of medium 1, is the matched load and is considered in Appendix A3.

8

a)

MEDIUM 1   MEDIUM 2   METAL

MEDIUM 1
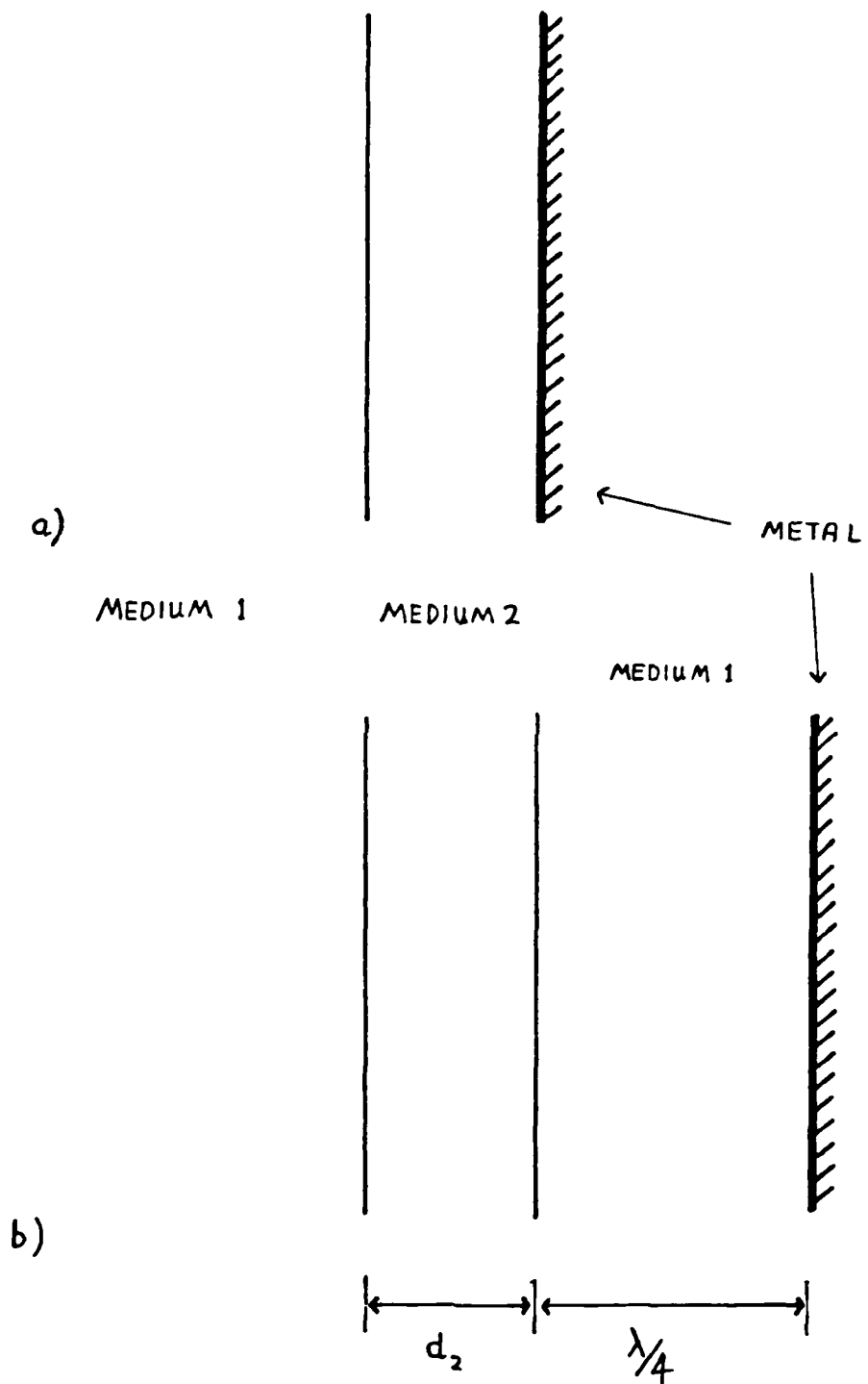
b)

d_2 $\lambda/4$

Fig 2.3   Termination of a layer of medium 2, of thickness, d_2, by
           a) a short circuit and b) an open circuit (assuming
           medium 1 is lossless)

3.   ABSORBER TYPES

3.1   General Requirements

It has been shown in the previous chapter that the reflection coefficient of a planar dielectric structure in free space, Γ, depends on the effective impedance, Z_L, that it presents to the incident wave,

$$\Gamma \ = \ \frac{Z_L - Z_o}{Z_L + Z_o} \tag{3.1}$$

and that the reflected power falls to zero if this impedance is matched to the impedance of free space, Z_o. (It is henceforth taken that medium 1 will always be free space.) It was pointed out in section 2.2 that a perfect impedance match could be obtained if the electric and magnetic material constants were identical,

$$\epsilon^* \ = \ \mu^* \tag{3.2}$$

and that the interface between such a material and free space would reflect no power. This condition on its own, however, is insufficient to make an electromagnetic absorber which is required to attenuate the wave as it propagates through it. The power in the wave decays with distance of propagation, x, according to the factor $\exp(-\alpha x)$. It is therefore required that the attenuation constant, α, be positive, and, if extinction of the wave is to be achieved in a reasonable thickness, it must also be large. Examination of equation (2.5) will show that, if α is to be non-zero, there must be an imaginary part to either or both of ϵ^* and μ^* - implying that the material must be lossy. Equation (2.5) is expanded in Appendix A2 in order to express α in terms of ϵ_r', μ_r', ϵ_r'' and μ_r'', giving

$$\alpha \ = \ - \sqrt{\epsilon_o \mu_o} \ \ \omega (a^2 + b^2)^{\frac{1}{2}} \ \sin(\tfrac{1}{2}\tan^{-1} -\tfrac{b}{a})$$

where $a = (\epsilon_r' \mu_r' - \epsilon_r'' \mu_r'')$ \hfill (3.3)

and $b = (\epsilon_r' \mu_r'' + \epsilon_r'' \mu_r')$.

Thus, in order to maximise α we require ε_r', ε_r'', μ_r' and μ_r'' all to be large, and this is in addition to the matching requirement, equation (3.2). Not surprisingly, materials meeting these requirements over wide frequency bands do not exist, and it is invariably necessary to employ one of the impedance matching strategies, described in the following sections.

3.2 Pyramidal Absorbers

Equation (2.11a) shows that the reflection coefficient at an abrupt interface between two media increases as the impedance difference between the two media increases. It might be expected, therefore, that the reflection is much reduced from a gradual impedance transition between the two materials, because the impedance difference between any two adjacent elemental layers will be small. Furthermore, the more gradual the transition, the lower the reflection becomes. One means of realising this gradual impedance transition is to shape the front surface of the absorber – arrays of pyramids or cones reminiscent of an egg-tray structure are common (see Figure 3.1). To be effective, the depth and periodicity of these pyramids or cones must be at least of the same order as the wavelength of the incident radiation, because, as the wavelength is increased above this, the interface appears more and more abrupt. This type of absorber, therefore, exhibits a low frequency cut-off dependent upon the dimensions of its surface texture, but offers a uniform high absorption level over a wide frequency range above this (Figure 3.6a), and is also found to work well over wide ranges of incidence angle. These desirable features make this type the usual choice for lining of microwave anechoic chambers. A range of sizes is commercially available for chambers of different lower operating frequency limits – pyramid depths of the order of 6 feet being required for operation down to below 1 GHz.
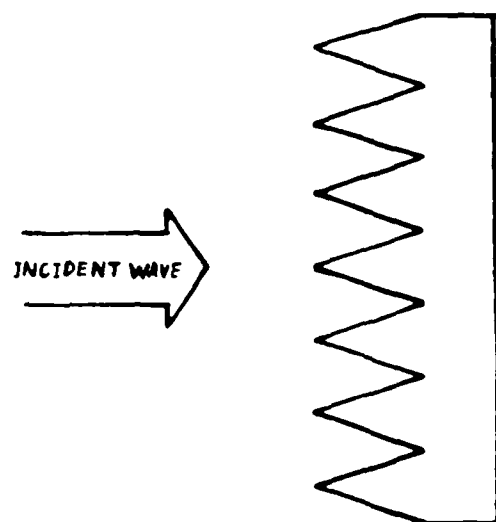
10

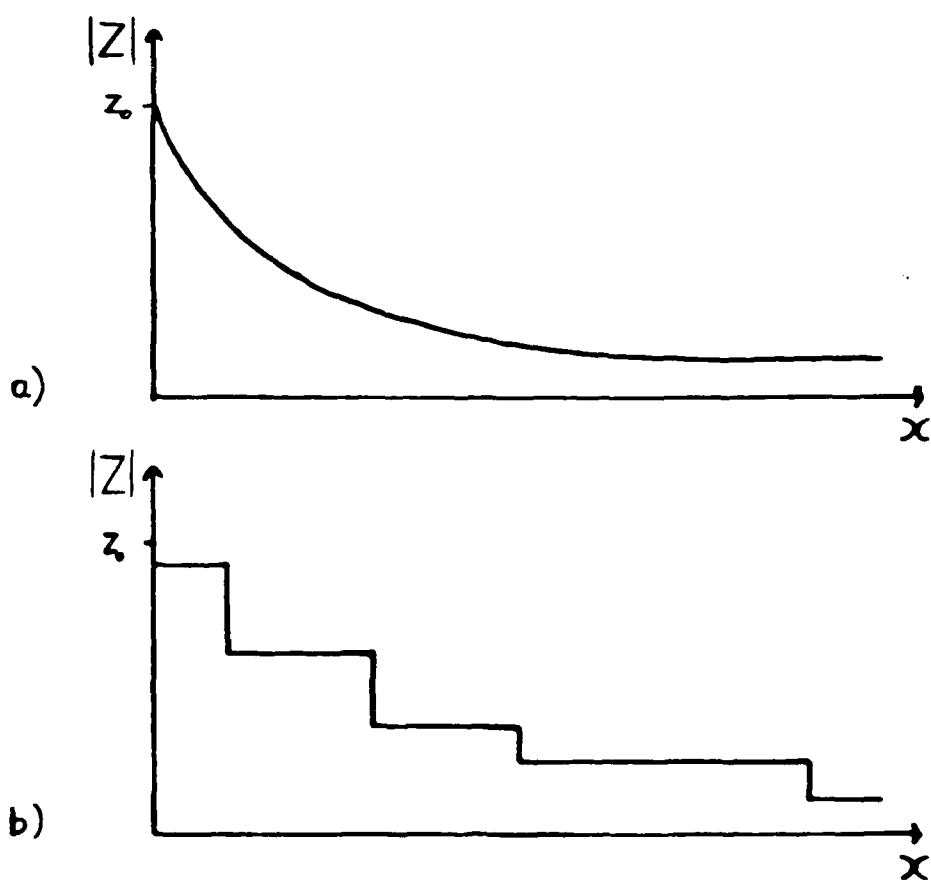Fig 3.1   A cross-sectional view of a pyramidal-type absorber

a)

b)

Fig 3.2   Impedance profiles, as functions of depth, for a) a smoothly
tapered, and b) a stepped, loading distribution

3.3 Tapered Loading

An alternative realisation of the gradual impedance transition is
the tapered loading. A low-loss matrix is loaded with a lossy material
in such a way that the concentration of the lossy component, and conse-
quently the magnitudes of the permittivity and permeability, increases
with depth, from a low level at the front face to a high level at the
back (Figure 3.2a). This may be achieved by loading an open-celled foam
or a three-dimensional plastic netting with a lossy fluid, either by
spraying from the back or by dipping and allowing to drain with the back
facing downwards. It is difficult, however, to control the impedance
distribution by these methods. An alternative approach, which overcomes
this problem, approximates the true gradual transition by means of series
of homogeneous layers of increasing loading, so that the impedance is a
stepped function of depth (Figure 3.2b). Good performance can be obtained
with as few as 3 layers of correctly chosen impedance and thickness
(Figure 3.6b). Examples of both of these types are commercially available,
providing broadband frequency coverage above a low frequency cut-off, in
the forms of either a flexible covering or a flat sheet. Usually, the
impedance transition region in these types is much smaller than is used
for the pyramidal types and performance is generally inferior. Nevertheless
their more convenient form makes them ideal in less critical applications.

3.4 Matching Layer

The principal disadvantage of the gradual impedance transition is
that the transition region must extend for at least one, and preferably
more, wavelengths, and this inevitably occupies space and adds weight –
especially at low frequencies. This disadvantage can be minimised by
reducing the transition region to a single thin layer of suitable
thickness and an impedance intermediate between those of the two media to
be matched (Figure 3.3). This principle is used in the application of
antireflection coatings to optical components, for which both media to be
matched are generally lossless. In this case, Z_1 and Z_3 are both real,
and a reflection coefficient of zero requires that the effective impedance
of the combined layers 2 and 3 (given by equation (2.12) with $Z_T = Z_3$) is

equal to Z_1, from which it follows that the matching layer must satisfy the condition:

$$Z_2 = \sqrt{Z_1 Z_3} \qquad \text{(a)}$$

and   (3.4)

$$|\tanh \gamma_2 d_2| = \infty \qquad \text{(b)}$$

The first condition requires that Z_2 also is real, so that the second reduces to $j \tan \beta_2 d_2 = j\infty$, which, according to equation (2.6), is satisfied when $d_2 = \lambda_2/4$ - ie when the thickness of the matching layer is equal to one quarter of the wavelength of the radiation in that layer. (The wavelength of a wave in a dielectric medium is not the same as the free space wavelength, λ_o, but is reduced by a factor which is dependent upon the electromagnetic material parameters of the medium - see Appendix A2.) It is thus evident that impedance matching by means of a single layer can be achieved only at the frequency for which the thickness criterion is satisfied. The savings in volume and weight that are gained by this means, therefore, are bought at the expense of limited bandwidth. In the microwave absorber case, medium 1 is free space so that Z_1 is real ($= Z_0$), but Z_3 is now complex, because medium 3 must be lossy. This greatly complicates the analysis and the selection of Z_2, γ_2 and d_2 is no longer as simple as indicated in equation (3.4). When the limited choice of actual materials is also considered, it is not surprising that, at microwave frequencies, approximate matching only is sought based upon an intermediate value of impedance, Z_2, and a quarter-wavelength thickness.

3.5 Tuned Layer

In all the methods described so far, it has been attempted to improve the impedance match between the absorbing layer and free space by the interposition of a transition layer. It is then assumed that the attenuation of the absorbing layer is great enough to completely attenuate the power of the wave in the available thickness. In the tuned layer, the imperfect match at the interface and the inadequate attenuation of the
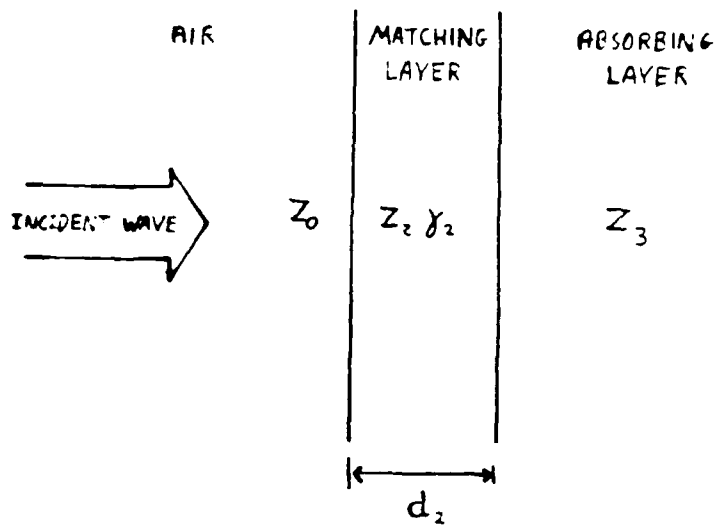
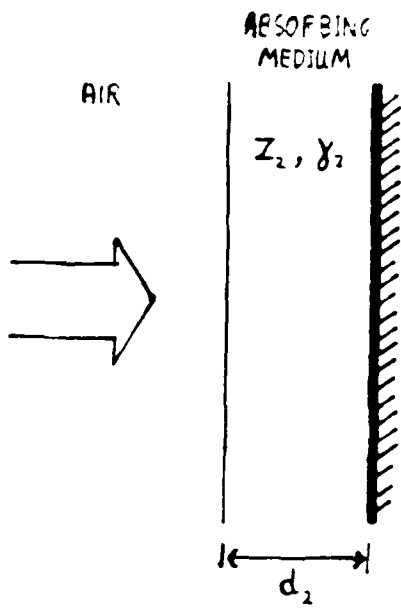Fig 3.3   A matching layer interposed between the air and the absorbing medium

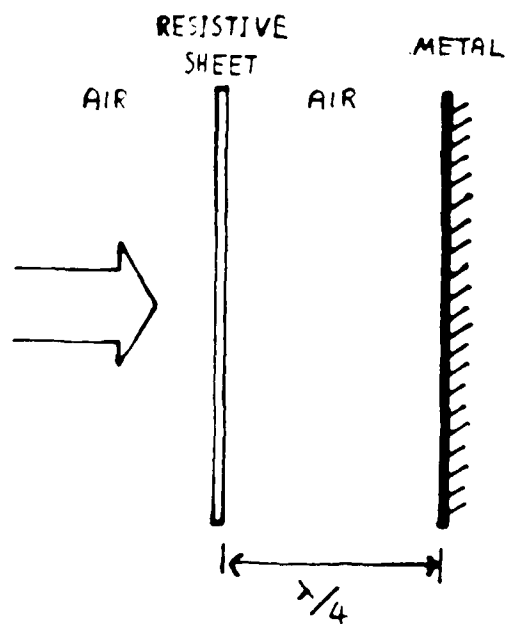Fig 3.4   The tuned layer absorber

Fig 3.5   The Salisbury screen absorber

layer are combined in such a way that their adverse effects cancel, while at the same time, the overall thickness is kept to an absolute minimum. These features make this type of absorber very popular despite the limited bandwidth which inevitably results from a tuned system. It is frequently referred to as a quarter-wave absorber, although this is, in fact, a misnomer as will become apparent. It consists, as shown in Figure 3.4, of a thin layer of lossy material, of thickness, d_2, impedance, Z_2, and propagation factor, γ_2, with a conductive backing. The effective impedance of this system is found, by equation (2.13), to be

$$Z_L = Z_2 \tanh \gamma_2 d_2 \qquad (3.5)$$

and it is evident from equation (2.11a) that, for zero reflection coefficient, we require

$$Z_L = Z_o \qquad (3.6)$$

Unfortunately, Z_L is complex whereas Z_o is, of course, real. Thus, for the perfect matching condition, it is necessary that the sum of the phase angles of the complex terms, Z_2 and $\tanh \gamma_2 d_2$, is zero while, at the same time the product of their magnitudes is equal to Z_o. In principle, this is possible, but it requires that 5 parameters, ε', ε'', μ', μ'' and d_2 simultaneously combine to satisfy both conditions. This is further complicated by the fact that all but d_2 are frequency dependent. A solution to this problem can, in principle, be found by optimisation techniques, but it can rarely be implemented using real materials. It is generally more useful to design a tuned layer for a known material using, for example, the method described in section 6.

The frequent but inappropriate use of the term "quarter-wave absorber" for this tuned layer arrangement stems from a simplistic view of its method of operation. According to this view, if the layer is a quarter wavelength thick, the portion of the incident wave that is transmitted at the front face re-emerges having undergone a phase-reversal due to reflection at the metal backing and an additional phase change of π due to its propagation along the half wavelength path through the layer and back again. Meanwhile, the directly reflected component has suffered only a phase-reversal on

13

reflection and so is in antiphase with the re-emergent component. These are then supposed to interfere destructively and, if the amplitudes of the two components are equal, complete cancellation occurs. There are two flaws in this argument. Firstly, the transmitted component, on re-emerging at the front face, undergoes partial reflection and partial transmission at the boundary so that a further partial wave is reflected back into the layer to emerge again at the front face (after a further phase reversal) in phase with the directly reflected component. This process, which is fully described in Appendix A3, repeats indefinitely as progressively smaller parts of the wave bounce within the layer. The total emergent wave, therefore, is composed of a sum of waves of decreasing amplitude, some of which are in phase and some phase-inverted, and all of these must add to zero if reflection is to be avoided. If the layer is lossy, then it may turn out that only the first re-emergent component is significant, but this leads into the second flaw. The argument given above has failed to take account of the phase changes that occur to both components when they are reflected at the front face and metal respectively. It is assumed that this is π in both cases, but it is apparent from section 2.2 that this will not be true for a lossy layer. The correct phase shifts for minimum reflection are therefore provided by a layer of thickness other than a quarter-wavelength. Understanding these inconsistencies in the simplistic view explains the apparent paradox which follows from it - namely that it is possible to achieve complete cancellation by using a lossless layer with suitable values of μ_r' and ϵ_r' where energy conservation considerations would prohibit this.

The approximate quarter wavelength condition refers, of course, to the reduced wavelength in the medium, λ_2, which is given in terms of λ_o by (see Appendix A2).

$$\lambda_2 = \lambda_o \cdot \frac{1}{(a^2+b^2)^{1/4}\cos(\tfrac{1}{2}\tan^{-1}-\frac{a}{b})} \qquad (3.7)$$

where

$$a = \epsilon_r'\mu_r' - \epsilon_r''\mu_r''$$

$$b = \epsilon_r''\mu_r' - \epsilon_r'\mu_r''$$

Thus, the larger the electromagnetic parameters are, the thinner can the absorber be made for a specified frequency provided, of course, that their values are also compatible with the requirements for impedance matching. Tuned, or narrowband absorbers of this type are commercially available and typically achieve a peak absorption in excess of 25 dB (see Appendix A4), and a bandwidth over which 10 dB absorption is achieved (10% power reflection) of 10-20% of the tuned frequency (Figure 3.6c). This performance at a tuned frequency in the region of 10 GHz (for which $\lambda_o = 30$ mm) can typically be provided by a sheet of 1.5-2 mm thickness.

3.6 Salisbury Screen

The Salisbury screen, patented in 1952 by W W Salisbury (4) is, like the tuned layer, a type of resonant absorber, but it is not reliant on the bulk permittivity and permeability of materials, and is therefore much easier to design. It consists of a resistive sheet parallel to and separated from a conducting plane by a quarter wavelength (Figure 3.5). The 1/4-wavelength air spaced conductor forms an open circuit (section 2.3) which appears in parallel with the resistive sheet. The effective impedance of the complete assembly, therefore, is simply the sheet resistance, which can be readily controlled and is generally frequency independent. If this is chosen to be 377 Ω per square, a good match to free space is achieved over the narrow frequency band for which the spacing is close to one quarter of the wavelength (Figure 3.6d). The main advantages of the Salisbury screen are its simplicity of design and production and its extremely light weight.

The spacing layer may be an air-filled foam with relative permittivity very close to 1, in which case the overall thickness will be $\lambda_o/4$. (The resistive layer itself must be very thin and its thickness can be neglected.) Alternatively, it is possible to reduce the overall thickness by using a lossless dielectric with a permittivity greater than 1, so that the wavelength in the spacing layer is reduced according to equation (3.7). Unfortunately, however, this carries with it the disadvantage of reduced bandwidth compared to the air spaced version.
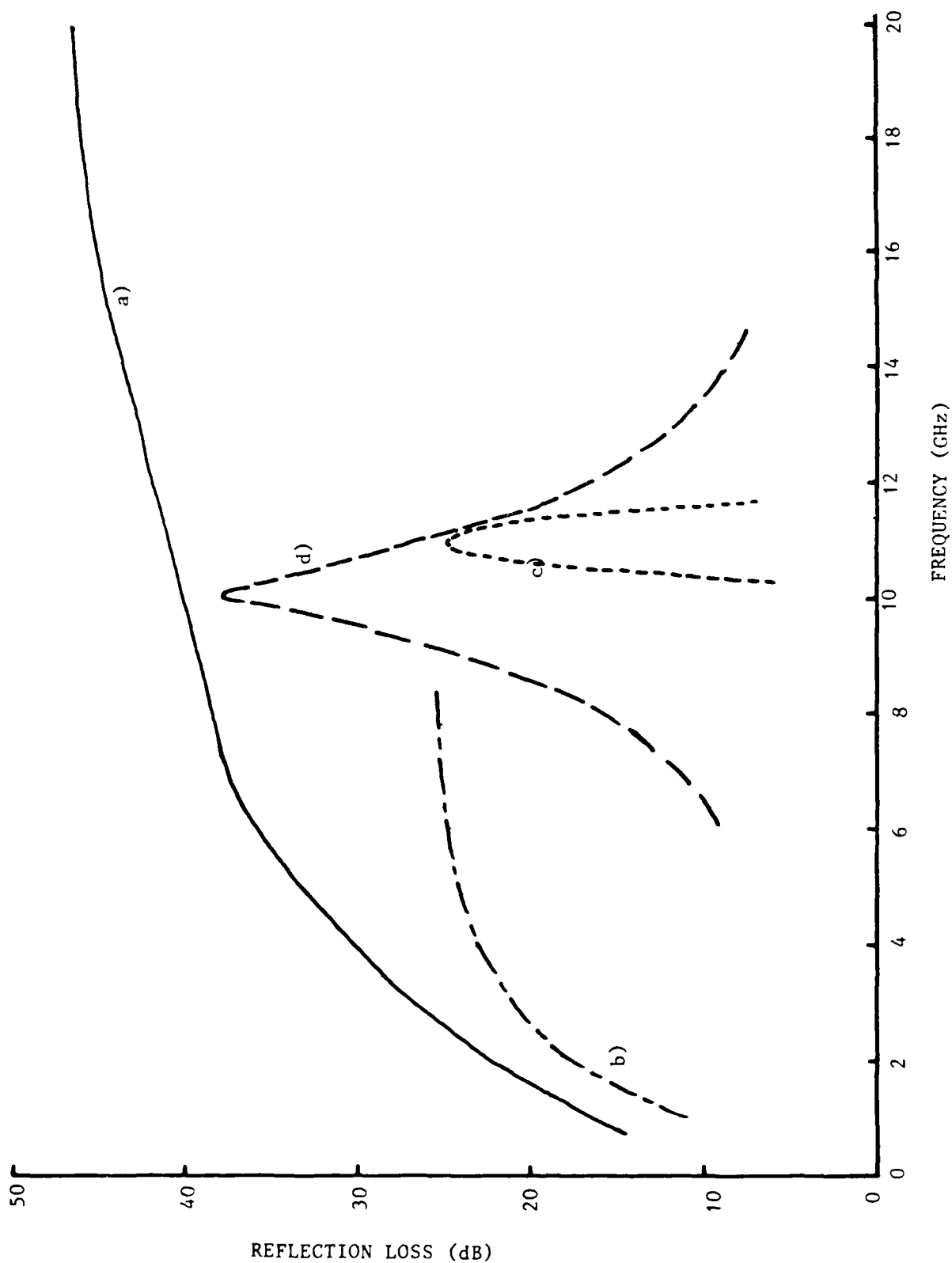
Fig 3.6   Some typical reflectivity spectra for the main types of RAM
a) A pyramidal absorber in carbon-loaded polyurethane foam with
   pyramid depth of 65 mm
b) A flat, stepped-loading foam absorber containing 3 layers
   with an overall thickness of 29 mm
c) A tuned layer 2.3 mm thick designed for 11 GHz operation and
d) A Salisbury screen absorber for 10 GHz consisting of a 377 Ω/
   square resistive sheet and a 7.5 mm air spacer

Alternatively, the Salisbury screen can be understood in terms of the standing wave pattern that is set up in the space in front of the metal reflector due to the interaction of the incident and reflected travelling waves (1). The maximum of the electric field standing wave occurs at a plane one quarter of a wavelength in front of the metal, and this is where the lossy dielectric element is located. The maximum of the magnetic field standing wave occurs at the metal boundary, and it might be expected that a magnetic analogue of the Salisbury screen could be constructed by locating a thin lossy magnetic element on the metal. This arrangement, if it could be realised, would be small, light-weight, convenient and would not rely on a frequency-sensitive spacing layer. Unfortunately, the corresponding magnetic property requirements cannot be met by available materials. The requirements are:

i. $\mu'' \gg \mu'$ at all frequencies of interest.

ii. $\mu'' \propto 1/\omega$ (without violating i).

The equivalent dielectric conditions are satisfied in the case of the resistive sheet because the dielectric loss of the sheet is furnished by its conductivity according to equation (2.3).

3.7 Techniques for Improving Bandwidth

It has been shown that broadband absorbers tend to be thick in order to accommodate the impedance graduation necessary to reduce surface reflections, while thin absorbers are generally narrowband because they rely on a thickness-related resonance. There is, however, considerable demand for improvements in bandwidth without incurring excessive thickness penalties. The standard method of extending the bandwidth of narrowband absorbers is by the use of multiple resonant layers. A carefully designed two-layer absorber can exhibit two loss peaks which can be arranged either to overlap, giving a single wider absorption band, or to cover two entirely separate narrow frequency bands. Further improvements can be gained with three or more layers, but with each new layer, the overall thickness is further increased. In the limit, as the number of layers

16

increases, the tapered loading wideband absorber is approached. In fact
it is common practice to approximate a defined impedance taper (eg expo-
nential) by means of a properly designed triple layer structure. The
design of multilayer absorbers is considered in section 6, but it will be
apparent that reliable information about the permittivity and permeability
of the constituent materials is of fundamental importance. This multiple
layer approach is also applicable to the Salisbury screen type of absorber,
with the advantage that design is less difficult, but the disadvantage
that the thickness build-up with increasing number of layers is more
severe. Nevertheless, such an absorber is described in reference (3).

A much neater solution to the problem of the thin broadband absorber
would make use of a single layer of a material whose electromagnetic
properties varied with frequency in such a way as to reduce the reflection
coefficient over a broader bandwidth. If such a material could be found,
not only would overall size be minimised, but the reflectivity would also
be less critically dependent on thickness. This material would need to
contain a lossy filler whose permittivity and permeability spectra were
carefully controlled, and might be realised by a suitable mixture of
available fillers. The Japanese have experimented with various combina-
tions of iron, ferrites, carbon and other materials on an empirical basis
(4), but a systematic approach would be heavily dependent on reliable
electromagnetic parameter data. Clearly this is a promising topic for
research. One further point concerning mixed loading is that the total
concentration of each component is less than would be the case if that
component were present alone. Consequently, the quantitative contribution
to the loss by each component will be reduced with the effect that band-
width improvement is achieved only at the expense of maximum loss - a high
narrow loss peak may be broadened, but it will also be flattened in the
process. Such a compromise, however, is probably quite acceptable in the
majority of applications, provided a reasonable reflectivity reduction
(say 10-13 dB) is maintained over this band.

It may also be possible to effect bandwidth improvements without unacceptable side effects by bringing into play entirely different concepts. For instance a rough front surface texture will tend to scatter incident radiation in all directions (if the dimensions of the surface texture are significant compared to the wavelength). This does not, of course, constitute absorption but it does reduce the specularly reflected signal. It may also prove advantageous to gain some measure of control over the effective impedance of a multilayer structure by judicious use of circuit analogue techniques. A periodic planar array of conducting elements, such as short narrow strips, crosses or discs present to an incident wave a complex impedance which depends upon the spacing and dimensions of these elements and the wavelength, and can be regarded as a circuit element in an electrical network model of the absorber (see section 6). The simplest example of this technique is, in fact, the Salisbury screen, for which the lumped impedance associated with the resistive sheet is real and frequency independent, but arrays of conductive elements permit frequency selective surfaces to be realised. The main advantages of this technique are that such frequency selective surfaces are easy to produce by metallic deposition through an appropriate mask and their size and weight are negligible.

4. MATERIALS FOR RAM

4.1 Composite RAM

In order for a microwave absorber to absorb electromagnetic energy in the frequency region of interest, it must contain a material which possesses an imaginary part to either or both of its permittivity and permeability. For most practical absorbers, however, it is nearly always necessary to make use of the electromagnetically lossy material in powder form dispersed in a suitable dielectric matrix, either because this is the only form in which the required properties are exhibited, or because the bulk form is inconvenient. To a first approximation, this matrix simply plays a mechanical and environmental role while the electromagnetic loss is furnished solely by the lossy filler. Nevertheless, in practice, the filler will modify the mechanical properties of the matrix and the matrix will dilute the electrical properties of the filler. The first of these effects is the province of the materials technologist while the second requires the expertise of an electromagnetic specialist.

There are various mixing laws which relate the effective electrical parameters of a composite material to those of its constituents. For particles which can be regarded as spherical – which includes most lossy fillers used in RAM – the dilution of permittivity is governed by a logarithmic law (5)

$$\ln\left|\varepsilon_c\right| = v \ln\left|\varepsilon_f\right| + (1-v) \ln\left|\varepsilon_b\right|$$

$$\delta_c = v\delta_F + (1-v) \delta_b$$

(4.1)

where $\left|\varepsilon\right|$ is the magnitude of the complex permittivity and δ is the phase angle. Here, the subscripts c, f and b refer to the composite, the filler and the binder respectively and v is the volume fraction of the filler in the final mixture. A similar pair of equations holds for the complex permeability. It is important to note that the electrical properties of a composite material, and consequently its electromagnetic response when deployed as an absorber, depend upon the volume composition and not, as

is often mistakenly assumed, on the composition by weight.

4.2 Binder Materials

The choice of binder material is determined by the intended application of the absorber. It is usually required that its electromagnetic material constants are small and frequency independent in the operating frequency range, so as to minimise the modification of the properties of the filler.

One of the simplest matrix materials, which is suitable for benign environmental conditions, is polyurethane foam. This is usually loaded with carbon black or fine graphite powder and, because carbon is non-magnetic, it is necessary to employ one of the impedance matching strategies described in chapter 3 in order to reduce surface reflectivity. Absorbers for microwave anechoic chambers are generally made from carbon-loaded polyurethane foam with a pyramidally shaped front face, because of its excellent wide band, wide angle electrical performance - the large size and poor environmental properties being comparatively unimportant in this application.

Where a strong radar echo must be reduced because a metal structure has been unavoidably located close to the transmitter (a common situation on ships), a thinner, more robust material is required. In these cases, however, the operating frequency is generally known and the usual solution is to coat the offending structure with a tuned absorber in the form of a magnetically loaded rubber or epoxy sheet. The selection of the exact polymer to be used as the matrix will depend on the environmental specifications, such as adhesion, temperature, rain erosion, deterioration due to sunlight, contaminants, abrasion or impact resistance. There is, currently, a considerable interest in liquid binders that can be applied by painting techniques, as this would greatly facilitate the application and maintenance of RAM coatings, especially on complex curved structures. Such a layer, however, would need to be at least 1-2 mm thick, which is enormous by conventional paint technology standards, and poses serious problems of composition, application and thickness control, which need to be solved before a practical RAM 'paint' can be developed.

Another area towards which current research efforts are directed is the development of structural RAM. The tuned layer is designed as a coating to be applied to a metallic structure, but an inherently absorbing structural material would be able to displace the metal, thereby eliminating the need for the coating and its associated maintenance. This places the additional requirement of mechanical strength on the material. Where only a lightweight panel is called for, capable of supporting its own weight or very light loads, a rigid plastic foam or a honeycomb structure, loaded with a suitable lossy material, might suffice. On the other hand, the member may be asked to support loads for which metal parts are normally used, and, for these situations, there is an interest in incorporating lossy fillers in fibre-reinforced composites.

It is thus evident that there is a wide range of mechanical and environmental requirements for RAM, and this leads to a wide range of matrix materials. Some examples have been mentioned in the preceding paragraphs, but many different specific situations could be envisaged whose special demands would necessitate special materials.

4.3 Lossy Fillers

Carbon powder is one of the most readily obtainable lossy fillers that is in common use. A carbon-loaded composite material acts by resistively dissipating the currents induced in it by the incident wave and thus provides a purely dielectric loss. As was mentioned in the last section, such a material, having no magnetic properties, inevitably presents an impedance mismatch to free space which must be countered by means of a suitable impedance transition layer. In a magnetically loaded matrix, however, such as the majority of commercially available tuned layers, these limitations are less severe. The addition of magnetic loss confers three main advantages. Firstly, the additional loss mechanism increases the attenuation constant, α, (equation (3.3)) compared to the dielectric only material. Secondly, the factor by which the free space wavelength is reduced in the material (equation (3.7)) is greater than it otherwise would be, so that a given wavelength is supported by a physically thinner layer. It is true that these objectives would also be served by a

21

non-magnetic dielectric with very large values of permittivity and dielectric loss, such as a ferroelectric, but this would magnify the impedance mismatch problem which is the substance of the third advantage of a magnetic dielectric. The combined magnetic and dielectric properties allow a much closer approach to the matching condition of equation (3.2), thereby considerably alleviating this problem. Thus the concept of a broadband absorber of reasonable thickness and without any transition regions, such as was suggested in section 3.1, assumes the possibility of a physical realisation. This is approached by solid sintered ferrite, which is commercially available in the form of ceramic tiles, 5-10 mm thick, that provide a reflectivity reduction of about 10 dB (10% power reflection) from below 100 MHz to 1-2 GHz, with a peak at a frequency between 200 and 800 MHz depending on composition and thickness. These tiles do, in fact, retain some resonant character, which serves to enhance their absorption over part of their operating bandwidth. Their high frequency performance is degraded because the magnetic constants of the ferrites decrease with increasing frequency in this region. Tuned layers for frequencies in the range 2-40 GHz generally use a dispersed powdered filler, such as carbonyl iron or a ferrite, in a polymer matrix. Although the magnetic parameters are reduced by the dilution, it is found that the optimum operating frequency range tends to increase, allowing ferrites, which in bulk form operate below 1 GHz, to be used in the microwave region. This type of absorber makes special use of the wavelength reduction property, and layers resonating in the region of 10 GHz can be produced in a thickness of only 1.5-2 mm, whereas the corresponding air-spaced Salisbury screen would have to be 7.5 mm thick.

The two major classes of magnetic fillers are metallic powders and the ferrites. The only metal powder in common use is carbonyl iron, which has been for many years the most widely used magnetic filler. It is produced by the pyrolysis of iron carbonyl and is readily available. There are other magnetic metal and alloy powders, such as cobalt and nickel, but these have not been widely explored for use in RAM. The other major class of magnetic filler, the ferrites, is considered in the following section.

4.4 Ferrites

The ferrites cover a very wide range of substituted iron oxides having a wide range of electrical and magnetic properties. The commonest class, the spinel ferrites, have a cubic crystal structure and can be represented by the general formula, MFe_2O_4, where M is usually a divalent transition metal ion, a combination of two or more such ions or alternatively a combination of mono- and tri-valent ions that maintains overall electrical neutrality. $MnFe_2O_4$, $Ni_xZn_{1-x}Fe_2O_4$ and $Li_xCr_{1-x}Fe_2O_4$ are examples of spinel ferrites. There is another class, usually containing large divalent metal ions such as Ba, Sr, Ca, or Pb, which crystallises into a hexagonal structure and these, too, may contain combinations of divalent or bi- and tetra-valent ions. Not only does the wide variety of compositions lead to a wide variation in the electromagnetic material constants of ferrites, but, even for a given composition, these properties are also dependent upon the microstructure of the material and hence on the precise details of its manufacture.

The general form of the relative permittivity and permeability spectra for iron and ferrites have the same general form and the characteristic features are illustrated in Figure 4.1.

The real part of the permeability, which has a constant low frequency value, μ_{1f}, falls to unity over a frequency band extending over approximately two decades, half of this reduction being achieved at the mid-point of this band, f_r. The magnetic loss rises to a peak, also at the frequency, f_r, but is small at frequencies above and below this band. This magnetic dispersion behaviour is very similar to the ideal dielectric relaxation described by Debye (6), and is the result of the progressive failure of the magnetisation (or polarisation in Debye theory) to follow the oscillations of the driving field as frequency is increased. Figure 4.1, however, shows that typical ferrites also exhibit a slight rise in the real part of the permeability at the low frequency end of the dispersion region and a corresponding dip at the high frequency end, which is indicative of a magnetic resonance phenomenon in addition to the relaxation (1a,7).
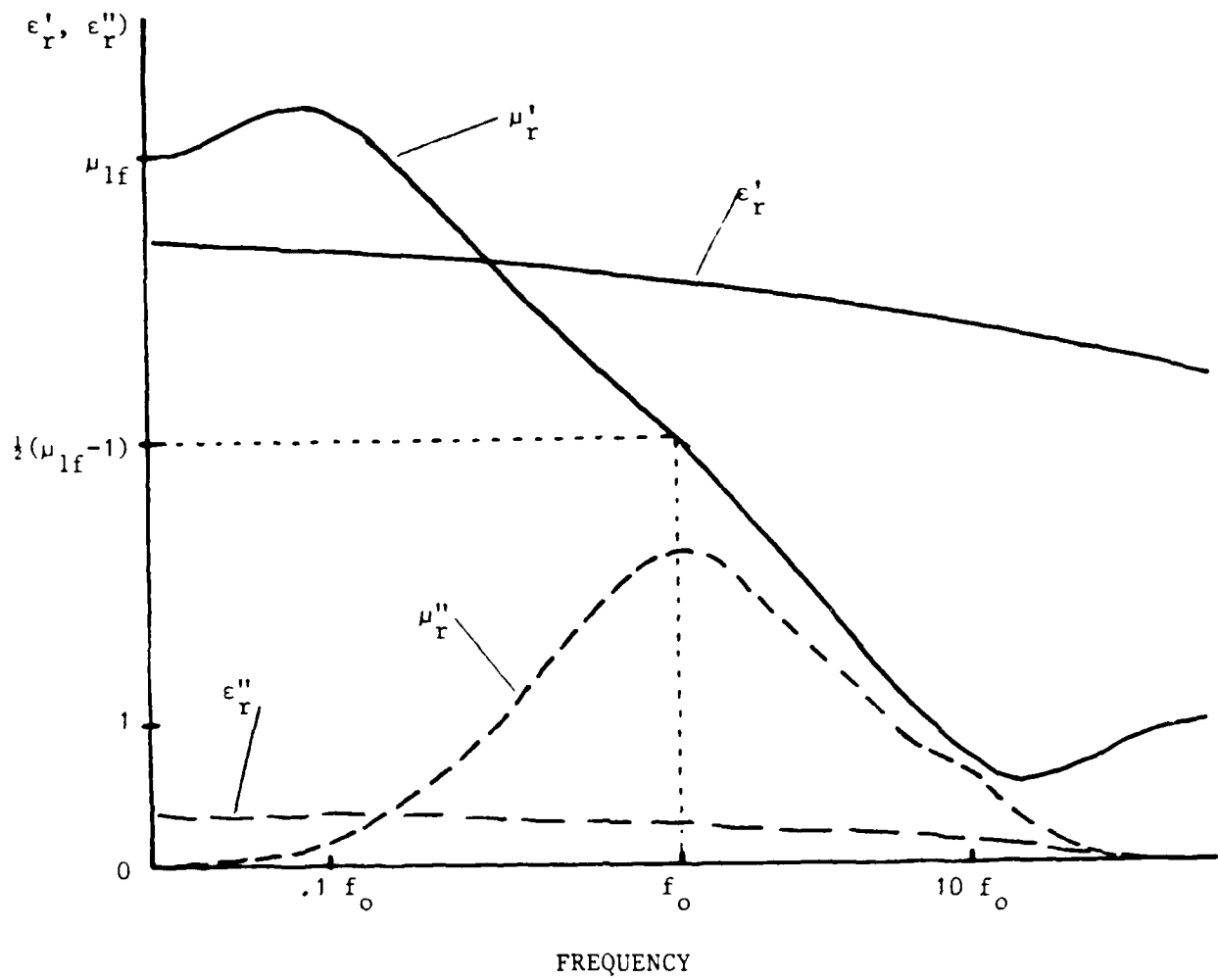
Fig 4.1   The general form of the electromagnetic material parameter
           spectra for ferrites

Moreover, the magnetic loss often displays a small secondary peak or, at least, a broadening, on the high frequency side of the relaxation dispersion which can lead to a small upper frequency extension of the useful operating band of absorbers in which they are incorporated. The real and imaginary parts of the complex permeability are in fact related to each other by a pair of transform relations known as the Kramers-Kronig relations, which are a fundamental result of the Causality Principle relating the magnetic response of a material to the field causing it (1a,8).

For spinel ferrites, μ_{1f} may typically lie in the range 10 to 1000 and f_r between 5 and 500 MHz. However, these two parameters are found not to be independent but are inversely related according to Snoek's empirical formula

$$\mu_{1f} \times f_r \approx \text{constant} \tag{4.2}$$

where the constant has a value of 5600 MHz. The occurrence of the dispersion region for spinel ferrites below 1 GHz accounts for their direct use, in the form of sintered tiles, as absorbers in this frequency region. For hexagonal ferrites, μ_{1f} is usually found to be somewhat lower (less than 30) and f_r somewhat higher (greater than 1 GHz) than the spinels, but the constant in equation (4.2) is found to be several times larger (typically 15-30 GHz). The microwave properties of some ferrites have been collected by von Aulock (7).

The permittivity, which is wholly independent of permeability, is found to vary with frequency much more slowly than the ideal Debye theory would predict. This is, in fact, typical of the dielectric behaviour of solids in general and is due to the greater variety of possible relaxation mechanisms and the greater degree of interaction between them. Nevertheless, the real and imaginary parts are also related by the Kramers-Kronig relationships. This general lack of correlation between the dielectric and magnetic spectra for ferrites, and indeed other magnetic-dielectric materials, is one reason why good thin broadband absorbers cannot be produced without recourse to impedance matching techniques.

5. MEASUREMENTS

It is essential to be able to measure the absorbing properties of an
absorber over the frequency band of interest. The usual approach is to use
free space methods and these are discussed in the first section of this chapter.
However, the reflection coefficient of an absorber is dependent upon the permit-
tivity and permeability of its constituent materials, so, in order to be able
to design absorbers, it is essential also to have the means of measuring these
parameters. In fact, because the same materials might be used in a range of
different frequency bands, the material parameter measurements are required to
span the whole of the microwave range. This problem is considered in the final
three sections of this chapter.

5.1 Reflectivity Measurement

It is obviously essential for the designer and his customer to be able
to assess the performance of an absorber. This is usually done by observing
the effect of the absorber on the propagation of microwave radiation in
free space, and the principle of the method is straightforward. The
performance of an absorber is defined in terms of the reduction in
reflected signal power compared to a perfectly conducting target of the
same size and shape. This implies that a two-part measurement is required –
first of all the return from the metal reference must be measured, followed
by the return from the absorber.

The basic arrangement is illustrated in Figure 5.1. The target is
usually chosen to be a flat square plate of side length equivalent to at
least several wavelengths, because this approximates most close v to the
infinite planar structure assumed by the theory (see chapters 2 and 3).
This is illuminated normally be means of a horn antenna, which is driven
by a microwave source via a reflectometer comprising a pair of back-to-
back directional couplers. A power sensor connected to the forward coupler
monitors the incident power and provides a reference signal. The reflected
signal is collected by the horn and measured by a second power sensor
connected to the take-off port of the reverse coupler. Assuming perfect
apparatus, the procedure is as follows. Firstly, the magnitude of the
reflection coefficient of the metal reference plate, Γ_m, is determined.
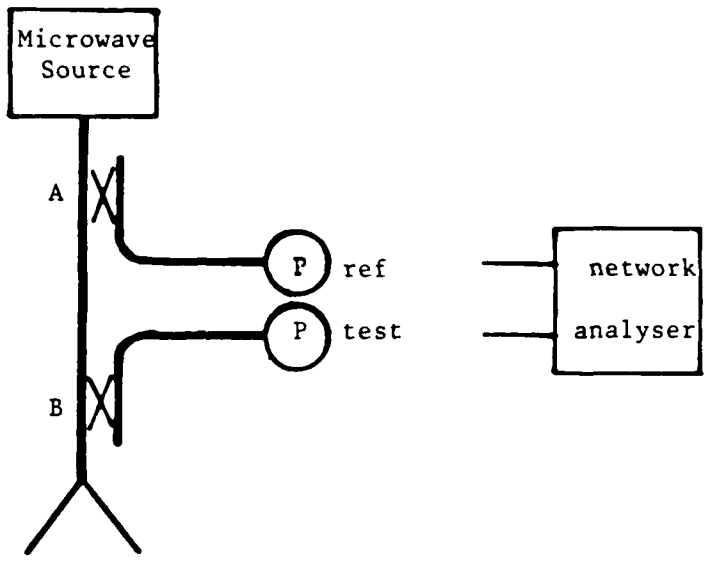
Fig 5.1   The reflectometer arrangement for making reflectivity measurements
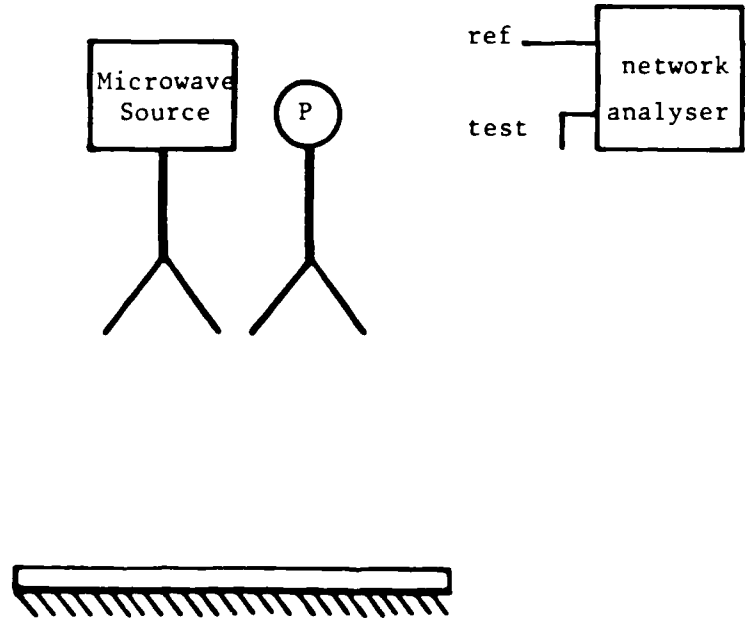

Fig 5.2   The two-horn arrangement for making reflectivity measurements
            in the transmission mode

If the incident and reflected power levels are P_i and P_m respectively, then

$$\Gamma_m = \frac{P_m}{P_i} \qquad . \tag{5.1}$$

Secondly, the reflection coefficient of the absorber, Γ_a, is determined in the same way and, if the reflected power in this case is P_a, then

$$\Gamma_a = \frac{P_a}{P_i} \qquad . \tag{5.2}$$

The reflectivity of the absorber, L, is then defined as the ratio of these two reflection coefficients

$$L = \frac{\Gamma_a}{\Gamma_m}$$

$$= \frac{P_a}{P_m} \tag{5.3}$$

which is more usually expressed in decibels (see Appendix A4) as

$$L_d = 10 \, \log_{10} \frac{P_a}{P_m} \, dB \qquad . \tag{5.4}$$

This is measured as a function of frequency over the band of interest and plotted as a reflectivity spectrum.

A number of experimental difficulties conspire to make the practical realisation of this measurement more complicated than the simplistic view above would indicate. Imperfect impedance matching between the microwave components gives rise to unwanted reflections whose phase relationships to the desired signal are not readily predictable and vary with frequency.

26

The imperfect directional properties of the couplers degrade their ability to isolate the return signal from the incident one. Non-ideal power detector characteristics lead to measurement errors which depend on power level and temperature. Fortunately, these problems can be overcome by using one of the commercially available network analysers. Scalar network analysers are automatic swept frequency systems which compensate for detector nonlinearities and mismatch and directivity errors by means of calibration and by averaging out the phase errors over the frequency sweep (9). Vector network analysers have the capability of measuring not only the relative amplitude, but also the phase difference between the two signals. This allows the error signals to be determined separately and then subtracted vectorially from the required measurements.

An alternative arrangement operates in the transmission mode making use of two separate horns (Figure 5.2), for illumination of the target and collection of the reflected power. This is often employed in conjunction with scalar network analysers as it reduces the directivity and mismatch errors, although it does suffer from direct horn-to-horn coupling. Another major advantage of this method is that the two horns can be separated in order to measure absorber performance at oblique angles of incidence, non-specular scattering, and, by independently rotating them, cross-polarisation effects.

5.2 Material Constant Measurement

The permittivity and permeability of materials are best measured by using samples mounted in a guided wave system, such as rectangular waveguide or co-axial line. Many methods are described in the literature but, because relatively few classes of materials are magnetic, most yield the permittivity only. It is usually feasible, however, to adapt these methods to take into account permeabilities other than unity. Nearly all of these methods can be divided into three categories: resonant, transmission line and time domain techniques.

A resonant cavity has a resonant frequency which is determined by its dimensions. If some dielectric material is inserted into this cavity, the resonant frequency will change by an amount depending on the properties and dimensions of the sample. It is possible to infer the electromagnetic properties of a material by observing the shift in resonant frequency of the cavity when an appropriately shaped sample is inserted. This technique has always been the main choice for precision measurements but suffers from the disadvantage that it is a spot frequency method. Parameter data for RAM design, on the other hand, is required to span a wide frequency range, and would therefore call for a large number of cavities, each tuned to a different frequency. It is for this reason that one of the other two techniques is usually chosen for the purpose of material characterisation for RAM.

5.3 Transmission Line Methods

These methods all rely on the measurement, in the frequency domain, of the reflection and/or transmission properties of a slab of material mounted in a transmission line. A transmission line is a guided wave system, usually of constant cross-section, which constrains electromagnetic waves to propagate along its length and inhibits any tendency to radiate outside its walls. These walls may comprise a boundary between two suitable dielectric materials, as is the case in optical fibres, but at microwave frequencies, and in the context of this chapter, they more usually take the form of metallic walls – either a single conductor such as circular or rectangular waveguide or a pair of conductors such as a co-axial line (Figure 5.3).

The properties of transmission lines are very similar to the properties of unbounded media developed in chapter 2, and, in fact, those unbounded systems can be treated as transmission lines without any walls as is done in chapter 6. In particular, reflection and transmission at an impedance discontinuity such as the junction between dielectrically filled and unfilled sections of line, are governed by very similar equations. Just as an unbounded medium has an intrinsic impedance dependent on the permittivity and permeability, so a transmission line has a characteristic impedance which depends additionally on its cross-sectional dimensions and the type

28

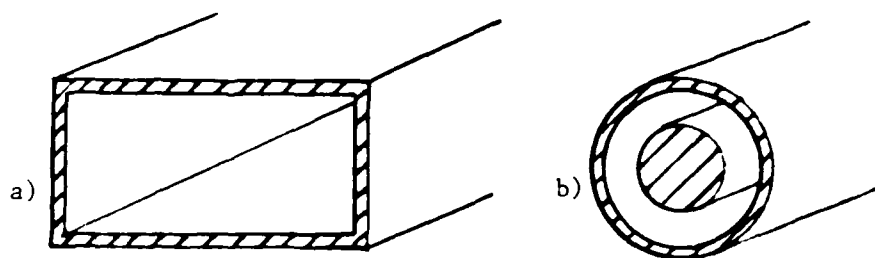Fig 5.3   Cross-sections of a) a rectangular waveguide and
           b) a co-axial transmission line
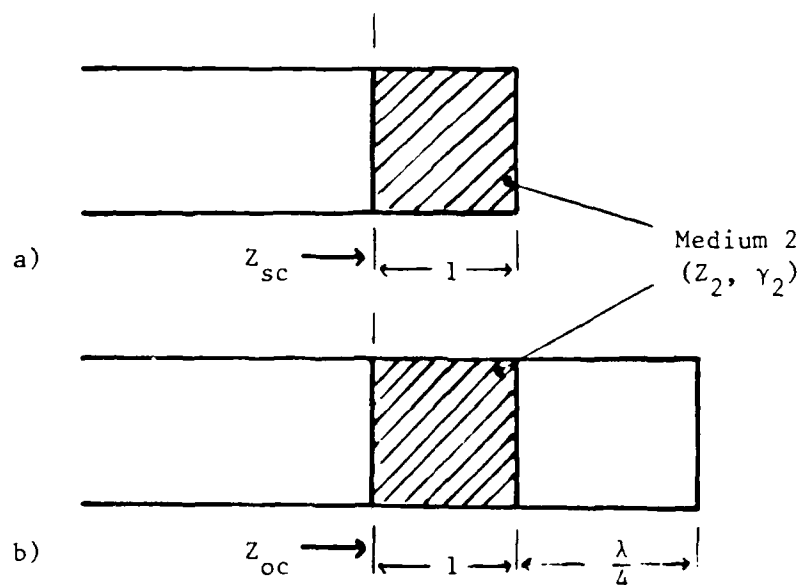

Fig 5.4   A section of material filled transmission line with
           a) a short circuit termination and b) an open circuit
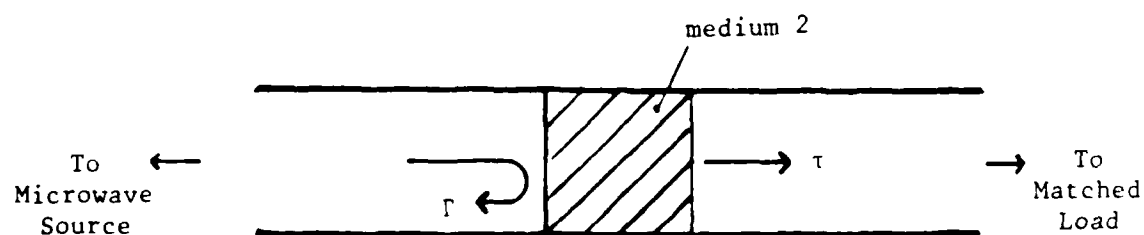   termination

Fig 5.5   A dielectric sample mounted in a section of transmission line
           for the measurement of both reflection and transmission
           coefficients

of mode propagating. Similarly, the propagation constant and the wavelength
are modified by mode-dependent dimensional factors. In the case of the
co-axial line, these factors become unity and the quantities have the
same values as the corresponding unbounded case. For simplicity, it will
be assumed for the remainder of this discussion that the transmission line
is co-axial - the treatment of single conductor waveguides can be pursued
in the references (1) if required.

It follows from this that the reflection coefficient at the junction
between a section of line and a load, Z_L, which may or may not include
another section of line, is given by equation (2.11c)

$$\Gamma = \frac{Z_L - Z_1}{Z_L + Z_1} \quad .$$

Also, the effective impedance of a section of material filled line of
length, 1, and terminated with a short circuit (Figure 5.4a) is

$$Z_{sc} = Z_2 \tanh \gamma_2 1 \tag{5.5}$$

where Z_2 and γ_2 are the characteristic impedance and propagation constant
of the line respectively. Similarly, with an open circuit termination,
(Figure 5.4b) the effective impedance is given by

$$Z_{oc} = Z_2 \coth \gamma_2 1 \tag{5.6}$$

and the open circuit is achieved, just as in the unbounded case of
section 2.3, by displacing the short circuit by a quarter wavelength of
lossless line.

Birks (10) in 1946, first described an experimental technique for the
measurement of both the dielectric and magnetic material parameters from
measurements of the open and short circuit impedance, and it became the
standard method for many years. It will be evident that equations (5.5)
and (5.6) together constitute a pair of complex simultaneous equations
which can be solved for the two complex quantities Z_2 and γ_2, from which,

29

in turn, the complex permittivity and permeability may be derived. By multiplying and dividing (5.5) and (5.6) we find

$$Z_2 = (Z_{sc} \cdot Z_{oc})^{\frac{1}{2}} \tag{5.7}$$

and

$$\tanh \gamma_2 l = (Z_{sc}/Z_{oc})^{\frac{1}{2}} \tag{5.8}$$

from which Z_2 is readily calculated. However, γ_2 must be deduced with the assistance of charts (11) and because the tanh function is periodic, there exists a series of solutions for γ_2. In order to resolve the ambiguity, it is necessary either to have some advance knowledge of the approximate values of μ_r^* and ε_r^*, or to repeat the measurement for a sample of different thickness and extract the only common solution. If a material is known to be non-magnetic ($\mu_r' = 1$, $\mu_r'' = 0$), then the complex permittivity can be determined from either the short or the open circuit measurement alone, or alternatively, the ambiguity inherent in the tanh function can be avoided by using only equation (5.7).

Birks measured the open and short circuit impe̤⁀ⁿ.es by observing the electric field standing wave pattern that is set up in the region in front of the sample due to the interference of the incident and reflected travelling waves (1). To do this, he used a slotted line. This is a section of transmission line with a longitudinal slot cut in its outer wall along which a probe may be moved in order to sense the electric field as a function of position (12). The two properties of the pattern that are of particular relevance are the ratio of the maximum to minimum amplitudes, known as the Voltage Standing Wave Ratio (VSWR), S, and the distance from the boundary of the first voltage minimum, x_o. The effective impedance, Z_L, seen at the boundary is then given by (1)

$$\frac{Z_L}{Z_1} = \frac{\frac{1}{S} - j \tan\beta_1 x_o}{1 - j \dfrac{\tan\beta_1 x_o}{S}} \tag{5.9}$$

where $\beta_1 = 2\pi/\lambda_1$ and λ_1 is the wavelength in the section of line in front of the sample. It is apparent that material parameters can be measured by

this method over a wide range of frequencies using the same apparatus,
but a large amount of adjustment of the slotted line and the open circuit
is necessary, making it a very time-consuming and painstaking exercise.
Another potential hazard, which is common to all transmission line methods,
is the error due to an imperfect fit of the sample into the guide. Any
air gaps between the sample and the guide walls can seriously affect the
reflection and transmission properties of that section of the guide and
extreme care is required in sample preparation. Despite these drawbacks,
the open and short circuit method can, with sufficient care, yield accurate
values of both permittivity and permeability over a broad range of micro-
wave frequencies.

The open circuit adjustment necessary in the open and short circuit
method can be avoided if the transmission coefficient can be accurately
measured. The filled section of line is inserted between two unfilled
sections with matched terminations to eliminate any unwanted reflections
(Figure 5.5). The reflection coefficient of this arrangement is shown
in Appendix A3 to be given by

$$\Gamma \;=\; \frac{r_1(1 - e^{-2\gamma_2 d})}{1 - r_1^2\, e^{-2\gamma_2 d}} \tag{5.10}$$

and the transmission coefficient by

$$\tau \;=\; \frac{e^{-\gamma_2 d}(1 - r_1^2)}{1 - r_1^2\, e^{-2\gamma_2 d}} \tag{5.11}$$

where r_1 is the reflection coefficient of the front interface, given by

$$r_1 \;=\; \frac{Z_2 - Z_o}{Z_2 + Z_0} \tag{5.12}$$

31

and Z_o is the characteristic impedance of the empty line. These two
equations can be solved simultaneously to yield γ_2 and r_1 from which μ_r^*
and ϵ_r^* may then be calculated. Once again, there is an ambiguity due to
the periodicity of the complex log function which must be resolved either
by means of a prior estimate or a second measurement with a different
sample thickness. Also, care must be exercised during sample preparation
to ensure a good fit in the guide.

Since Birks first devised his method, advances in microwave instru-
mentation have led to the development of the network analyser, which is
able to measure the reflection and transmission coefficients of an unknown
network without the need to make physical adjustments. The addition of a
computer, an analogue-to-digital converter and a programmable frequency
source then allows wide-band material parameter measurements to be made
automatically. This is a vast improvement on Birks' original method and
provides a rapid, wide-band measurement facility, capable of generating
a comprehensive material data-base for absorber design.

5.4   Time Domain Methods

In the frequency domain, the response function, $R(j\omega)$, from a linear
network excited by an input function, $V(j\omega)$, is given by

$$R(j\omega) \;=\; H_1(j\omega) \times V(j\omega) \tag{5.13}$$

where $H_1(j\omega)$ is the frequency response of the network. In the present
case the network consists of the sample in a transmission line, the input
function is the incident wave and the response function is either the
reflected or the transmitted wave. The frequency response is the reflec-
tion or transmission coefficient spectrum and is determined, as described
in the previous section, by applying sinusoidal input signals at a range
of frequencies, ω, and measuring the resulting responses. It is also
possible to deduce this information by time domain methods. In this case,
the input is a fast rising step waveform $V(t)$, which, according to Fourier
analysis, may be regarded as the sum of an infinite series of continuous
sine waves of appropriate amplitude and phase, covering a very wide range
of frequencies. (The ideal step waveform with zero rise-time would contain

32

all frequencies from 0 to ∞). The response r(t), then takes the form of
a transient waveform with a gradual decay, and this can be analysed as a
similar infinite series of sine-waves each of which represents the
response of the network to the corresponding input. In fact, the fre-
quency domain functions, V and R, are related to their time domain
counterparts, v and r, by the Fourier transform, F, thus (13):

$$V(j\omega) \ = \ F(v(t)) \ = \ \int_{\infty}^{\infty} v(t) \ e^{-j\omega t} \cdot dt$$

and
<div align="right">(5.14)</div>

$$R(j\omega) \ = \ F(r(t)) \ = \ \int_{\infty}^{\infty} r(t) \ e^{-j\omega t} \ dt$$

Thus, it is possible to derive the frequency response directly from
measurements of the input waveform and its response waveform

$$H_1(j\omega) \ = \ \frac{F(r(t))}{F(v(t))} \tag{5.15}$$

The permittivity and permeability can then be found by the same means as
described in the previous section.

A typical reflection arrangement is shown in Figure 5.6a which shows
a sample-filled section of transmission line terminated by a short circuit.
This is excited by a fast pulse generator and the line is monitored by a
sampling gate connected to some form of recording device (oscilloscope,
XY recorder or computer). Because the pulse propagates down the line at
a finite velocity, the sampler is able to resolve in time the incident
and the various reflected wavefronts. The form of the response that
would be seen by the sampler is shown in Figure 5.6b, where the features
are correlated with the sequence of reflection events giving rise to them
(Figure 5.6c). (This phenomenon of diminishing part-waves bouncing from
end to end within the sample is also described with reference to the
frequency domain in Appendix A3.) The first event to be seen (A) is the
incident step, followed by its reflection (B) from the front face of the

<div align="center">33</div>
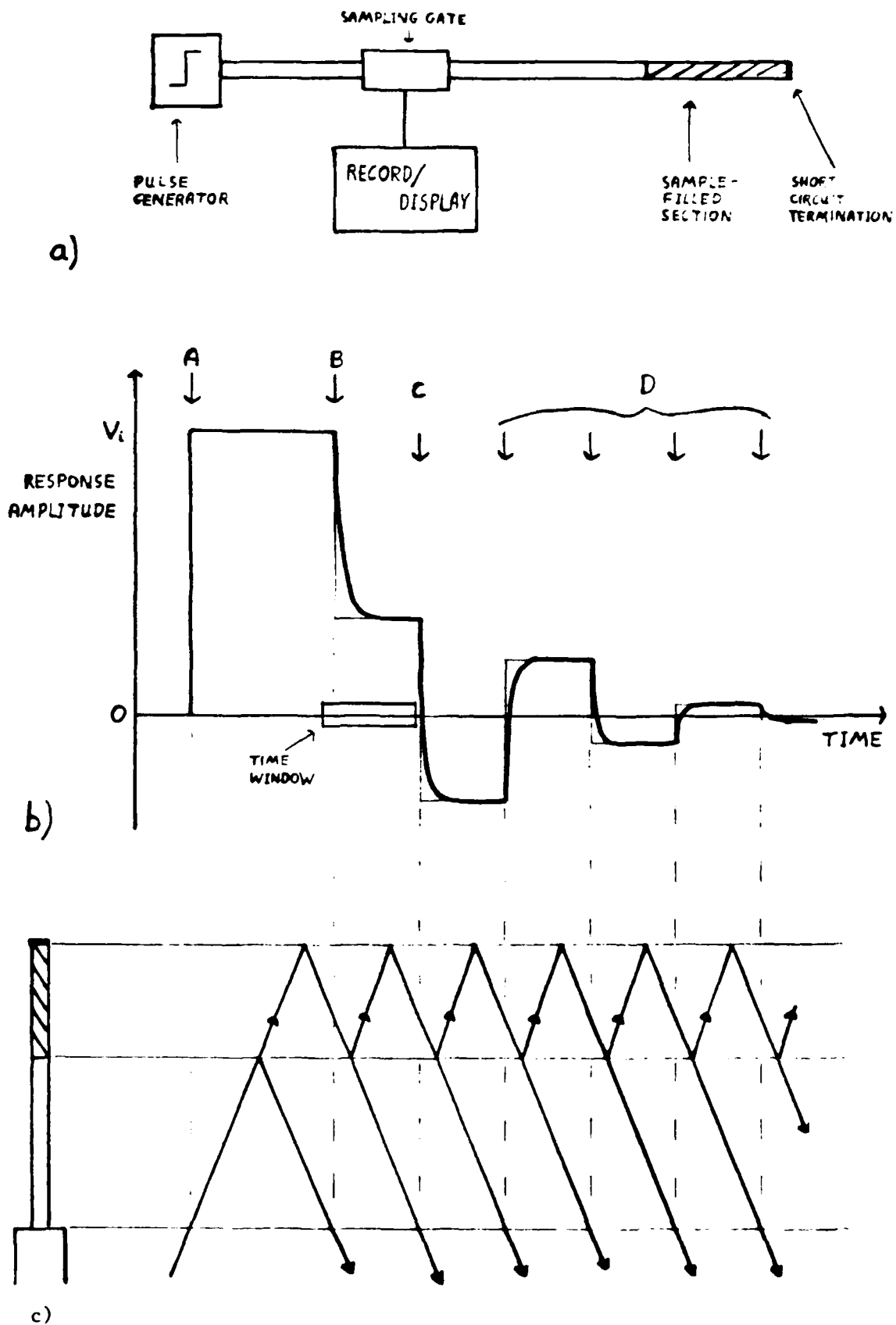
Fig 5.6   a) The basic experimental arrangement for TDS measurements
             with a short-circuited sample
          b) The form of the voltage response seen at the sampling gate,
             showing the time window isolating the front face reflection
          c) The sequence of reflection events giving rise to the response
             shown in b)

sample after a delay corresponding to the transit time from sampling gate to sample and back again. The magnitude of this reflection is determined by the front boundary reflection coefficient which is given by equation (5.12). Because insertions of a dielectric medium into a line reduces its characteristic impedance below that of the empty line, Z_2 is less than unity so that the reflection coefficient, and consequently the reflected step, is negative. After a further delay, while the step propagates along the length of the sample in both directions, the reflection from the back face of the boundary (also negative) (C) is seen. In fact, when this particular wavefront reaches the front face, part of it is transmitted back towards the sampling gate, while the remainder is re-reflected back into the sample, where progressively diminishing part waves are reflected between the two end faces, giving rise to all the subsequent reflections (D) until it has completely decayed away. This example made use of a short circuit termination but an open circuit or matched load could equally well have been connected. In these cases, the rear face reflection coefficient would have been either +1 or 0 respectively, rather than −1. This would affect reflections C and D, causing the measured voltage to tend towards $2V_i$ or V_i respectively, rather than 0, where V_i is the amplitude of the incident step. Note, however, that the steps A and B are independent of termination.

Time Domain Spectroscopy (TDS) is the generic name by which these time domain methods of measuring electromagnetic material parameters are known, and the topic has been reviewed by van Gemert (13), Cole (14) and Mishra et al (15). Two basic approaches can be distinguished depending upon whether the sample relaxation time is long or short compared to the transit time within the sample. It is the second of these that is illustrated in Figure 5.6b. It will be noticed that, although the input step waveform has been assumed to have a negligible rise-time, the steps reflected from the sample each exhibit a significant decay – this is due to the variation with frequency of the reflection coefficient, and hence of the dielectric and magnetic properties of the material. The figure shows that these decays are essentially complete before the next reflected wavefront arrives at the sampling gate, which is the case if the sample is sufficiently long to delay its arrival for several decay time-constants.

In this case, known as the single reflection case, the time window of the sampling gate can be restricted so that it includes only this decay, as shown in Figure 5.6b, and the rear face can then be ignored. The network then being investigated is the front boundary of the sample only and the observed response is the step response of the front boundary reflection coefficient given by equation (5.12). In the alternative approach, the sample length is short so that the response decay is far from complete before the arrival of the next reflection. It is now necessary to open out the time window to include the whole response, which is that resulting from the total reflection coefficient of a finite sample and includes all the re-reflected part-waves as described in Appendix A3.

Although conceptually simpler, the single reflection method suffers from the disadvantage that very long samples are required in order to delay subsequent reflections as much as possible. Clearly, cutting off the observed decay limits the information available at long times and hence at low frequencies. However, it is often found, in practice, that the low frequency limit is determined by the transit time, on the length of line in front of the sample, of unwanted reflections due to the impedance mismatch between line and sampling gate. The practical lower limit for the single reflection method is found to be about 100 MHz, although the total reflection approach, which is generally easier to use, remains valid down to about 1 MHz. The upper frequency limit in both methods is, in principle, limited by the high frequency content of the input waveform, which depends upon how fast a rise-time can be achieved. Current tunnel diode pulse generations are capable of producing a pulse with a rise time of 30-40 ps, which should be sufficient to yield results up to 20 GHz. In practice, however, high frequency performance is limited to much lower frequencies by timing errors. When equation (5.15) is applied, it is important to ensure that the two waveforms both have the same time reference. However, because these two waveforms are recorded separately, (once with the sample in place and once with a short circuit located at the position of the front face), it is difficult to achieve this to better than an error of 2 ps, which limits the maximum useful frequency to about 3 GHz. Special time referencing procedures can be employed to reduce this error to about 0.4 ps, allowing useful measurements to be made up to 10 to 15 GHz, but the accuracy of results for high permittivity/permeability

materials is better in the single reflection method (16).

The fortunes of the time domain and frequency domain approaches have changed over the years with the development of microwave technology. The original advantage of time domain techniques was that a wide frequency range could be covered in a single rapid measurement, so that results could be obtained much faster than in the frequency domain, where separate measurements must be made at a series of discrete frequencies. This was particularly attractive when automatic network analysers were expensive and slotted lines were the standard technique. However, the Fourier transformation of the time domain data into the frequency domain adds some delay in the presentation of results and degrades their accuracy due to the uncertainties in time origin for the two integrations, especially at the higher frequencies. Reduction of these timing errors can extend the high frequency limit of time domain measurements to about 15 GHz, but this adds considerably to the equipment cost which becomes comparable to that of some of the automatic network analysers (ANAs) available nowadays. A less sophisticated time domain system, however, might prove to be cost effective at frequencies below a few GHz, and might complement an ANA operating between 2 and 18 GHz. For the highest precision in ANAs, the recently introduced Hewlett Packard 8510 can be used over the entire frequency range from 50 MHz to 26 GHz, but at double the capital cost. Unfortunately, there is no cheap way of making the wide-band material parameter measurements necessary for a systematic approach to RAM design.

6.   ABSORBER DESIGN

The design of even a simple type of electromagnetic absorber cannot,
unfortunately, be reduced to a straightforward set of equations, yielding a
set of values for the material parameters and layer dimensions, given a parti-
cular performance requirement. Even if this were possible, the limited range
of material parameters offered by real materials would make it extremely
unlikely that such a solution could be realised. In order to design an
absorber systematically, therefore, the converse approach must be adopted –
its performance must be predicted for a given set of material parameters and
layer dimensions, and these must be refined by iteration. This chapter
describes one general model for this purpose, although others could be devised.

6.1   Transmission Line Model

The most general absorber configuration that can be envisaged consists
of multiple planar layers of different homogeneous isotropic materials.
By a suitable choice of the total number, material properties and thick-
nesses of the layers, most of the types described in chapter 3 can be
represented. Furthermore, this configuration can also readily be modelled
by a series of unbounded transmission line segments connected in cascade
(Figure 6.1). Each segment has a characteristic impedance and propagation
constant defined by the intrinsic impedance and propagation constant of
the medium of the corresponding layer, and the segment length is given by
the layer thickness.

The model may be further simplified by treating each transmission
line segment as a 4-terminal network and the electric and magnetic fields
at each interface as voltages and currents, as shown in Figure 6.2.
According to network theory, the voltages and currents at the input and
output terminals are uniquely related by a set of coefficients character-
istic of the particular network (17), thus

$$v_1 = A_{11}v_2 + A_{12}(-i_2)$$

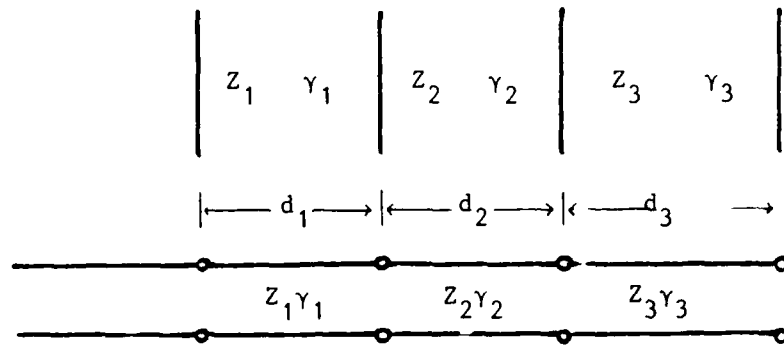$$i_1 = A_{21}v_2 + A_{22}(-i_2)$$

$$(6.1)$$

Fig 6.1   An arbitrary multilayer absorber and its transmission line analogue

Fig 6.2   A 4-terminal network showing the sign convention used for the input
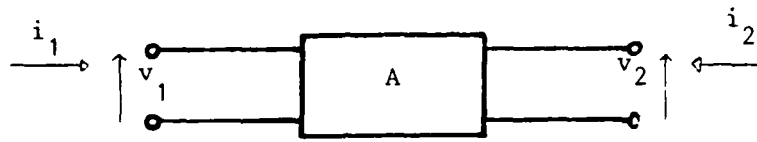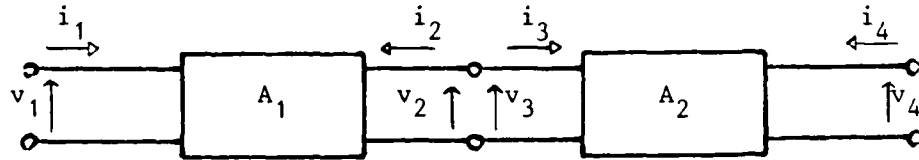   and output voltages and currents

Fig 6.3   A pair of 4-terminal networks connected in cascade
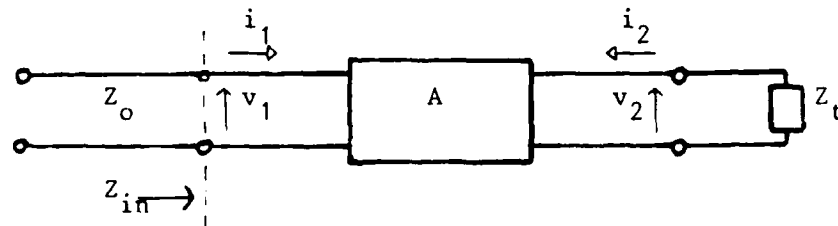
Fig 6.4   A 4-terminal network with a load connected to its output terminals
           and a section of transmission line connected to its input
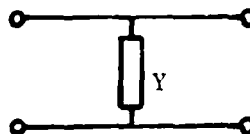
Fig 6.5   A 4-terminal network consisting of a lumped admittance connected
           across the line

This may be rewritten in matrix form

$$\begin{bmatrix} v_1 \\ i_1 \end{bmatrix} = A \begin{bmatrix} v_2 \\ -i_2 \end{bmatrix} \qquad (6.2)$$

where

$$A = \begin{bmatrix} A_{11} & A_{12} \\ A_{21} & A_{22} \end{bmatrix} \qquad (6.3)$$

is the cascading matrix of the network (also called the transformation, general circuit parameter, A or ABCD matrix).

If two such networks, A_1 and A_2, are connected in cascade as shown in Figure 6.3, equation (6.2) may be applied independently to each. This gives

$$\begin{bmatrix} v_1 \\ i_1 \end{bmatrix} = A_1 \begin{bmatrix} v_2 \\ -i_2 \end{bmatrix} \qquad \text{and} \qquad \begin{bmatrix} v_3 \\ i_3 \end{bmatrix} = A_2 \begin{bmatrix} v_4 \\ -i_4 \end{bmatrix}$$

However, it is apparent by inspection that

$$v_3 = v_2 \qquad \text{and} \qquad i_3 = -i_2$$

from which it follows that

$$\begin{bmatrix} v_1 \\ i_1 \end{bmatrix} = (A_1 \times A_2) \cdot \begin{bmatrix} v_4 \\ -i_4 \end{bmatrix} \qquad (6.4)$$

The same procedure may be repeated for three or more networks in cascade. This demonstrates the important principle that a series of n cascaded 4-terminal networks can be reduced to a single equivalent network, simply

38

by multiplying together (in the correct order) the individual cascading matrices

$$A = A_1 \times A_2 \times A_3 \times \ldots \ldots A_n \qquad (6.5)$$

If a network, A, is terminated by an impedance, Z_t, as shown in Figure 6.4, the output voltage and current must satisfy

$$Z_t = \frac{v_2}{-i_2} \qquad (6.6)$$

The effective input impedance of this arrangement, looking into the input terminals of the network, can similarly be written as

$$Z_{in} = \frac{v_1}{i_1} \qquad (6.7)$$

Expanding this using equation (6.1) and substituting equation (6.6), the input impedance can be expressed as

$$Z_{in} = \frac{A_{11}Z_t + A_{12}}{A_{21}Z_t + A_{22}} \qquad (6.8)$$

If this terminated network is now cascaded with a section of transmission line of characteristic impedance Z_o, the reflection coefficient, Γ, is given by

$$\Gamma = \frac{Z_{in} - Z_o}{Z_{in} + Z_o} \qquad (6.9)$$

Thus, if the cascading matrix elements are known as functions of frequency for each layer of a general multilayer absorber, and if it has a known termination, Z_t, the reflection loss spectrum can be calculated with the aid of equations (6.9), (6.8) and (6.5). In practical absorbers, the termination usually consists of either an intimate metal backing plane or

39

no backing at all, which can be represented as a short circuit ($Z_t = 0$) or a matched load ($Z_t = Z_o$) respectively.

6.2 Matrix Elements

It is a well-known result of network theory, that the cascading matrix for a length, d, of transmission line having characteristic impedance, Z, and propagation constant, γ, is

$$A = \begin{bmatrix} \cos\alpha & jZ \sin\alpha \\ j/Z \sin\alpha & \cos\alpha \end{bmatrix} \qquad (6.10)$$

where

$$\alpha = j\gamma d \qquad . \qquad (6.11)$$

Here, Z is simply the intrinsic impedance of the medium given by equation (2.7) and γ is the propagation constant given by equation (2.5). These matrix elements are therefore readily calculated if the complex permittivity and permeability and the thickness of the layer are known.

A further advantage of this model is that the 4-terminal networks of which it is composed are not restricted to transmission line segments. It is therefore possible to incorporate any absorber structure which can be represented by a 4-terminal equivalent network whose cascading matrix elements can be determined. An important practical example of this is the resistive sheet used in the Salisbury screen absorber, which can be expressed as a lumped admittance, Y, connected across the line as shown in Figure 6.5. The cascading matrix for this network is

$$A = \begin{bmatrix} 1 & 0 \\ Y & 1 \end{bmatrix} \qquad (6.12)$$

where

40

$$Y = \frac{1}{R_s} \qquad\qquad (6.13)$$

and R_s is the sheet resistance of the resistive layer.

As was mentioned in chapter 3, it is possible to exercise some additional control over absorber properties by incorporating one or more frequency selective surfaces, each consisting of a planar array of conductive elements of suitably chosen shape, dimensions and spacing. There exists in the literature equivalent circuit representations for many of these, including arrays of strips, crosses, circular and square rings and Jerusalem crosses (18). The equivalent circuit allows the effective lumped admittance of the frequency selective surface, $Y(f)$, to be expressed as a function of frequency, whereupon it may be treated as a 4-terminal network of the type shown in Figure 6.5 and described by equation (6.12).

6.3 Oblique Incidence

A practical absorber will generally be required to operate for angles of incidence other than normal, which has been considered exclusively so far. The model can be modified to take into account oblique incidence simply by placing a slightly different interpretation on the cascading matrix elements. In the case of the layer of homogeneous material, the model assumes a guided wave propagating along the axis of the transmission line, which can be directly related to the physical situation in which a plane wave is propagating normal to the layer boundary. If the plane wave is propagating at an angle, θ, to this direction, as shown in Figure 6.6, then the guided wave in the model becomes the component of the plane wave resolved in the direction perpendicular to the plane of the interface. Thus α in equation (6.10) becomes $\alpha \cos\theta$ and the characteristic impedance of the line, Z, which is given by the ratio of the parallel components of the electric and magnetic fields becomes either $Z/\cos\theta$ or $Z\cos\theta$, depending on whether the incident electric field is polarised perpendicular or parallel to the plane of incidence (Figure 6.6a and b respectively).
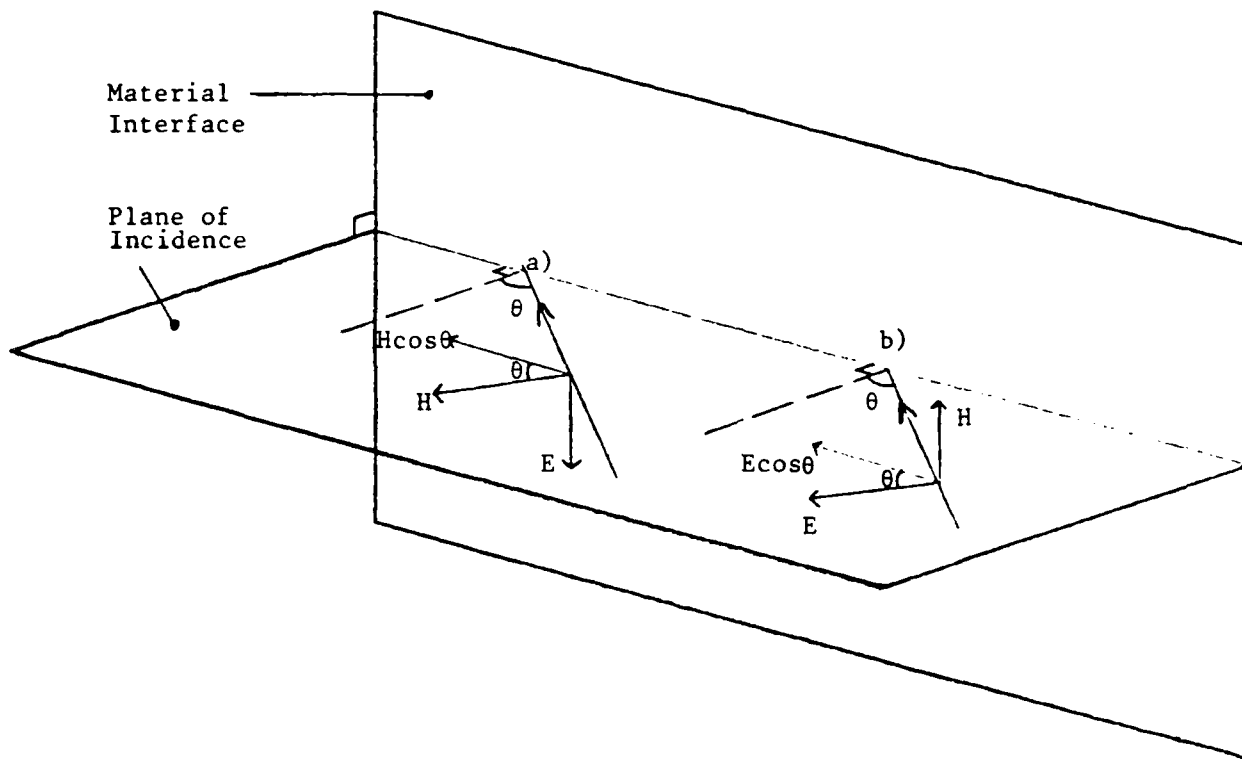
Fig 6.6   A pair of waves obliquely incident on a material interface showing the
           field components resolved parallel to the interface. In a), the
           electric field is polarised perpendicular to the plane of incidence,
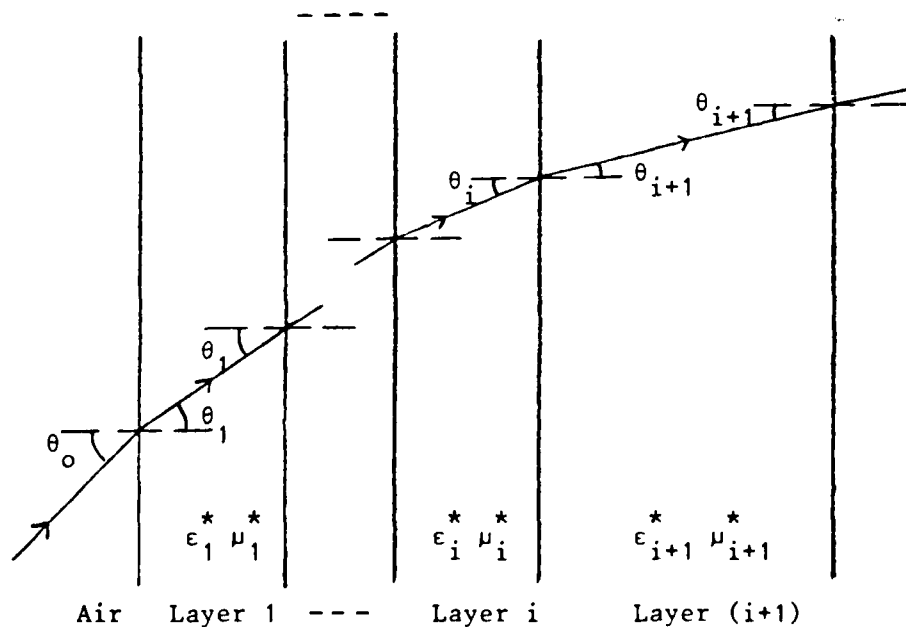   while in b) it is parallel

Fig 6.7   Oblique incidence in a multilayer absorber structure

In a multilayer structure (Figure 6.7), the angle of incidence, θ_i, at the boundary between layers i and (i+1) can be obtained by repeated application of Snell's Law at each interface. Snell's Law states that

$$\sqrt{\varepsilon_i^* \mu_i^*} \, \sin\theta_i \;\; = \;\; \sqrt{\varepsilon_{i+1}^* \mu_{i+1}^*} \, \sin\theta_{i+1} \tag{6.14}$$

where ε^* and μ^* are the relative complex permittivity and permeability of each layer. It therefore follows that

$$\cos\theta_i \;\; = \;\; \left(1 - \frac{1}{\varepsilon_i^* \mu_i^*} \sin^2\theta_o \right)^{\frac{1}{2}} \tag{6.15}$$

where θ_o is the angle of incidence at the front face of the entire multilayer structure.

In the case of lumped admittance layers, it is also necessary to resolve the incident plane wave into perpendicular and parallel components for use in the transmission line model. However, care must be taken in the treatment of frequency selective surfaces. Their equivalent circuits are usually only strictly valid for normal incidence, but in many cases, they may be approximately true over a limited range of incidence angles. If the layer is buried in a medium having large values of ε_i^* and μ_i^*, then, according to equation (6.15), the incidence angle on the surface itself, θ_i, will be significantly less than the incidence angle at the front face of the absorber, θ_o, and the equivalent circuit may be useful for most incidence angles of practical interest.

6.4 Design of Absorbers

It is not difficult to implement the transmission line model described in this chapter as a computer program to produce a versatile design aid for electromagnetic absorbers. A configuration appropriate to any given application may be selected from the basic types described in chapter 3, from a simple single layer to a complex multilayer design. If the layer thicknesses are specified and the properties of each layer are known over the frequency range of interest, the reflectivity spectrum may be predicted.

For homogeneous layers, the materials will be chosen on the basis of the criteria of chapter 4 and their electromagnetic parameters can be measured by the techniques of chapter 5. If frequency selective surfaces are to be incorporated, their equivalent lumped admittance must be determined as a function of frequency from the appropriate equivalent circuit, taking into account the properties of the medium in which they are embedded. Finally, individual properties may be varied at will in order to refine the performance of the design and to assess the effect of such variations that may occur as a result of manufacturing tolerances.

7.   REFERENCES

(1)a.   A von Hippel, "Dielectrics and Waves", Wiley, 1954.

   b.   J D Kraus and K R Carver, "Electromagnetics", McGraw-Hill (2nd ed), 1973.

(2)   W W Salisbury, US Patent 2 599 944 (1952).

(3)   T M Connolly, E J Luoma, US Patent 4 038 660 (1977).

(4)   US Patent 4 116 906 (1978); Japanese Patents 54 041 495 (1979), 54 110 497 (1979), 54 127 000 (1979), 54 152 402 (1978).

(5)   P S Neelakantaswamy, B V R Chowdari, A Rajaratnam, J Phys D 16 1785-99 (1983).

(6)   P Debye, "Polar Molecules", Dover, 1945.

(7)   W H von Aulock, "Handbook of Microwave Ferrite Materials", Academic Press, 1965.

(8)   G W Chantry, "Long Wave Optics, Vol I, Principles", Academic Press, 1984 (pp 214-221, 399-401).

(9)a.   P Lacy, Microwave Journal, 25, (April 1982), p 57.

   b.   P Spenky, W Foster, ibid, p 83.

(10)   J B Birks, Proc. Phys. Soc. (London), 60, 282-292, (1948).

(11)   A E Kennelly, "Chart Atlas of Complex Hyperbolic and Circular Functions", Harvard University Press, 1914.

(12)   A B Giordano, "Measurement of Standing Wave Ratio", ch. 2 in M Sucher, J Fox (Eds) "Handbook of Microwave Measurements, Vol 1", Polytechnic Press of Polytechnic Institute of Brooklyn, 1963.

(13)   M J C van Gemert, Philips Res. Repts. 28, 530-572 (1973).

(14)   R H Cole, Ann. Rev. Phys. Chem. 28 283-300 (1977).

(15)   R K Mishra, S S Chaudhary, A Swarup, J. Sci. & Ind. Res: 42 548-556
        (1983).

(16)   C Gabriel, A W J Dawkins, R J Sheppard, E H Grant, J. Phys. E 12
        513-516 (1984).

(17)   J L Altman, "Microwave Circuits", van Norstrand (1964).

(18)   I Anderson, Bell. Syst. Tech. J. 54 1725-31 (1975); IEE Colloq. on
        "Multiband Techniques for Reflector Antennas", Oct 28, 1983;
        R J Langley, E A Parker, Electronic Lett. 18 294-6 (1982).

APPENDIX A1.   THE EFFECTIVE IMPEDANCE OF MULTILAYERED STRUCTURES

In order to determine the effective impedance, Z_L, of a layered structure in terms of the parameters of the individual layers, the problem must be broken down as illustrated in Figure A1.1. The overall layered structure is considered as a 3-layer structure comprising medium 1, the layer of medium 2 of thickness, d_2, characteristic impedance, Z_2, and propagation factor, γ_2, and the remaining layers are regarded as a terminating impedance Z_T.

The electric field in layer 2 may be considered to be the resultant of two electric field waves, the incident wave E_{i2} travelling in the +x direction and the reflected wave, E_{r2}, travelling in the -x direction. If the electric fields at the 2-3 interface ($x = 0$) are $E_{i2}(0)$ and $E_{r2}(0)$ (both of which are understood to include the time variation term $e^{j\omega t}$ implicitly), the two waves can be described thus

$$E_{i2}(x) = E_{i2}(0)\, e^{-\gamma_2 x} \tag{A1.1}$$

$$E_{r2}(x) = r_{23}\, E_{i2}(0)\, e^{+\gamma_2 x} \tag{A1.2}$$

where the complex reflection coefficient at the 2-3 interface is given by

$$r_{23} = \frac{Z_T - Z_2}{Z_T + Z_2} = \frac{E_{r2}(0)}{E_{i2}(0)} \tag{A1.3}$$

Thus the net electric field at an arbitrary point x in layer 2 is given by the sum of the two waves:

$$E_2(x) = E_{i2}(0)(e^{-\gamma_2 x} + r_{23}\, e^{+\gamma_2 x}) \tag{A1.4}$$

An analogous line of argument can be applied to the magnetic fields, and noting also that $\underline{E}$ and $\underline{H}$ are uniquely related by the characteristic impedance of the medium, Z_2, according to equation (2.6), this yields:
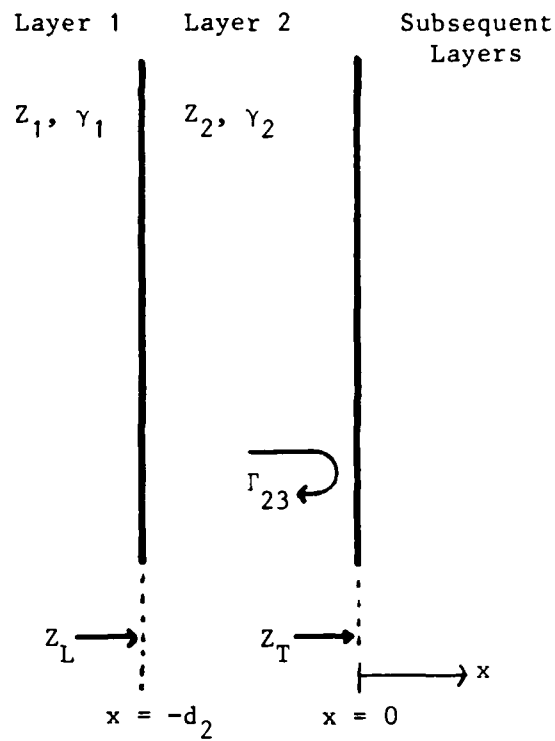
Fig A1.1   The effective input impedance, Z_L, of a layer terminated
with a layer or combination of layers having an effective
input impedance, Z_T

$$H_2(x) = \frac{E_{i2}(0)}{Z_2} (e^{-\gamma_2 x} - r_{23} e^{+\gamma_2 x}) \tag{A1.5}$$

Now, the impedance at any point x in layer 2 is simply obtained by dividing (A1.4) and (A1.5) thus

$$Z(x) = \frac{E(x)}{H(x)} = Z_2 \frac{e^{-\gamma_2 x} + r_{23} e^{\gamma_2 x}}{e^{-\gamma_2 x} - r_{23} e^{\gamma_2 x}} \tag{A1.6}$$

In particular, this can be evaluated at the 1-2 interface ($x = -d_2$), at which point $Z(x)$ is equal to the effective impedance, Z_L, of the entire multilayer structures and substituting for r_{23} from (A1.3), this becomes

$$Z_L = Z_2 \frac{(Z_T + Z_2) e^{\gamma_2 d_2} + (Z_T - Z_2) e^{-\gamma_2 d_2}}{(Z_T + Z_2) e^{\gamma_2 d_2} - (Z_T - Z_2) e^{-\gamma_2 d_2}}$$

$$\tag{A1.7}$$

$$= Z_2 \frac{Z_T + Z_2 \tanh \gamma_2 d_2}{Z_2 + Z_T \tanh \gamma_2 d_2}$$

The terminating impedance Z_T can be determined in terms of its constituent layers by repeating the same procedure for layer 3 and so on.

APPENDIX A2.   PROPAGATION AND WAVELENGTH IN LOSSY MEDIA

The propagation constant, γ, can be expressed in terms of the relative material constants of the medium, ϵ_r^* and μ_r^*:

$$\gamma = j\omega\sqrt{\epsilon_r^*\mu_r^* \cdot \epsilon_o\mu_o} \qquad (A2.1)$$

which can be rearranged to separate the magnitude and phase components:

$$\gamma = j\omega\sqrt{\epsilon_o\mu_o}\ (a^2 + b^2)^{1/4}\ \exp\ j(\tfrac{1}{2}\tan^{-1}(-b/a)) \qquad (A2.2)$$

where $\quad a = \epsilon_r'\mu_r' - \epsilon_r''\mu_r''$

and $\quad b = \epsilon_r''\mu_r' + \epsilon_r'\mu_r''$

The propagation constant can also be expressed in terms of the attenuation constant, α, and phase constant, β, of the medium:

$$\gamma = \alpha + j\beta \qquad (A2.3)$$

Equating the real and imaginary parts of (A2.2) and (A2.4) leads to

$$\alpha = -\omega\sqrt{\epsilon_o\mu_o} \cdot (a^2 + b^2)^{1/4}\ \sin(\tfrac{1}{2}\tan^{-1}(-b/a)) \qquad (A2.4)$$

and

$$\beta = \omega\sqrt{\epsilon_o\mu_o} \cdot (a^2 + b^2)^{1/4}\ \cos(\tfrac{1}{2}\tan^{-1}(-b/a))\ . \qquad (A2.5)$$

Since

$$\beta = \frac{2\pi}{\lambda}\ , \qquad (A2.6)$$

it is possible, with the help of (A2.5) to express the wavelength in terms of the frequency and the electromagnetic material parameters.

In free space, where $\varepsilon_r' = \mu_r' = 1$ and $\varepsilon_r'' = \mu_r'' = 0$, the free space wavelength, λ_o, of a wave of angular frequency, ω, is found to be

$$\lambda_o = \frac{2\pi}{\omega\sqrt{\varepsilon_o\mu_o}} \tag{A2.7}$$

(This also follows from the relationship $\sqrt{\varepsilon_o\mu_o} = 1/c$ where c is the velocity of light.)

The same wave propagating in a lossy medium has a wavelength, λ_m, given by

$$\lambda_m = \frac{2\pi}{\beta_m} \tag{A2.8}$$

Thus the wavelength of a wave in a lossy medium is reduced below the free space wavelength by the factor given by

$$\frac{\lambda_m}{\lambda_o} = \frac{1}{(a^2+b^2)^{1/4}\cos(\tfrac{1}{2}\tan^{-1}(-b/a))} \tag{A2.9}$$

In the case of a lossless medium ($\varepsilon_r'' = \mu_r'' = 0$) this simplifies to the familiar expression

$$\frac{\lambda_m}{\lambda_o} = \frac{1}{\sqrt{\varepsilon_r'\mu_r'}} \quad . \tag{A2.10}$$

APPENDIX A3.   DIELECTRIC SLAB SANDWICHED BETWEEN TWO MEDIA

In this appendix the behaviour of an electromagnetic wave is considered in a slab of dielectric material, of impedance, Z, propagation constant γ and thickness d, which is bounded at the front by an infinite extent of medium 1 (impedance Z_1), and at the back, by an infinite extent of medium 3 (impedance Z_3). This is illustrated in Figure A3.1 which shows the successive reflections at the boundaries, and the signal amplitude and phase at each point. The incident wave, E_o, is understood to include the time variant factor, $e^{j\omega t}$.

When the incident beam strikes the front face, a fraction, r_1, of it is reflected and a fraction, $(1 - r_1)$, is transmitted, where r_1 is the boundary reflection coefficient given by

$$r_1 = \frac{Z - Z_1}{Z + Z_1} \qquad (A3.1)$$

The transmitted portion propagates to the second interface, suffering attenuation and phase shift according to the propagation constant, γ, which, as the figure shows, is equivalent to muliplication by $e^{-\gamma d}$. Here it is again partly reflected and partly transmitted, but this time the boundary reflection coefficient is

$$r_2 = \frac{Z_3 - Z}{Z_3 + Z} \qquad (A3.2)$$

The reflected portion then propagates back again to the front interface, suffering further attenuation and phase shift, where another partial reflection and partial transmission occurs. At this point the direction of propagation is from medium 2 to medium 1, so the reflection coefficient is $-r_1$. This process continues until the internally reflected wave has diminished to insignificant levels and it is evident that the total reflected and transmitted waves each comprise a series of partial beams. The reflected wave, E_r, therefore, is given by the sum of the reflected partial beams

MEDIUM 1　　　MEDIUM 2　　　MEDIUM 3

Z_1 , γ_1　　　Z , γ　　　Z_3 , γ_3

$r_1 \leftarrow$　　　$r_2 \leftarrow$

$\rightarrow -r_1$

d

E_0　　　$(1-r_1)E_0$

$r_1 E_0$

$(1-r_1)E_0 e^{-\gamma d}$

$(1-r_2)(1-r_1)E_0 e^{-\gamma d}$

$r_2(1-r_1)E_0 e^{-\gamma d}$

$(1+r_1)r_2(1-r_1)E_0 e^{-2\gamma d}$　　$r_2(1-r_1)E_0 e^{-2\gamma d}$

$(-r_1)r_2(1-r_1)E_0 e^{-2\gamma d}$　　$(-r_1)r_2(1-r_1)E_0 e^{-3\gamma d}$

$(1-r_2)(-r_1)r_2(1-r_1)E_0 e^{-3\gamma d}$

$(1+r_1)(-r_1)r_2^2(1-r_1)E_0 e^{-4\gamma d}$　$(-r_1)r_2^2(1-r_1)E_0 e^{-4\gamma d}$

$(-r_1)r_2^2(1-r_1)E_0 e^{-3\gamma d}$

$(-r_1)^2 r_2^2(1-r_1)E_0 e^{-4\gamma d}$　$(-r_1)^2 r_2^2(1-r_1)E_0 e^{-5\gamma d}$

$(1-r_2)(-r_1)^2 r_2^2(1-r_1)E_0 e^{-5\gamma d}$

$(1+r_1)(-r_1)^2 r_2^3(1-r_1)E_0 e^{-6\gamma d}$　$(-r_1)^2 r_2^3(1-r_1)E_0 e^{-6\gamma d}$

$(-r_1)^2 r_2^3(1-r_1)E_0 e^{-5\gamma d}$
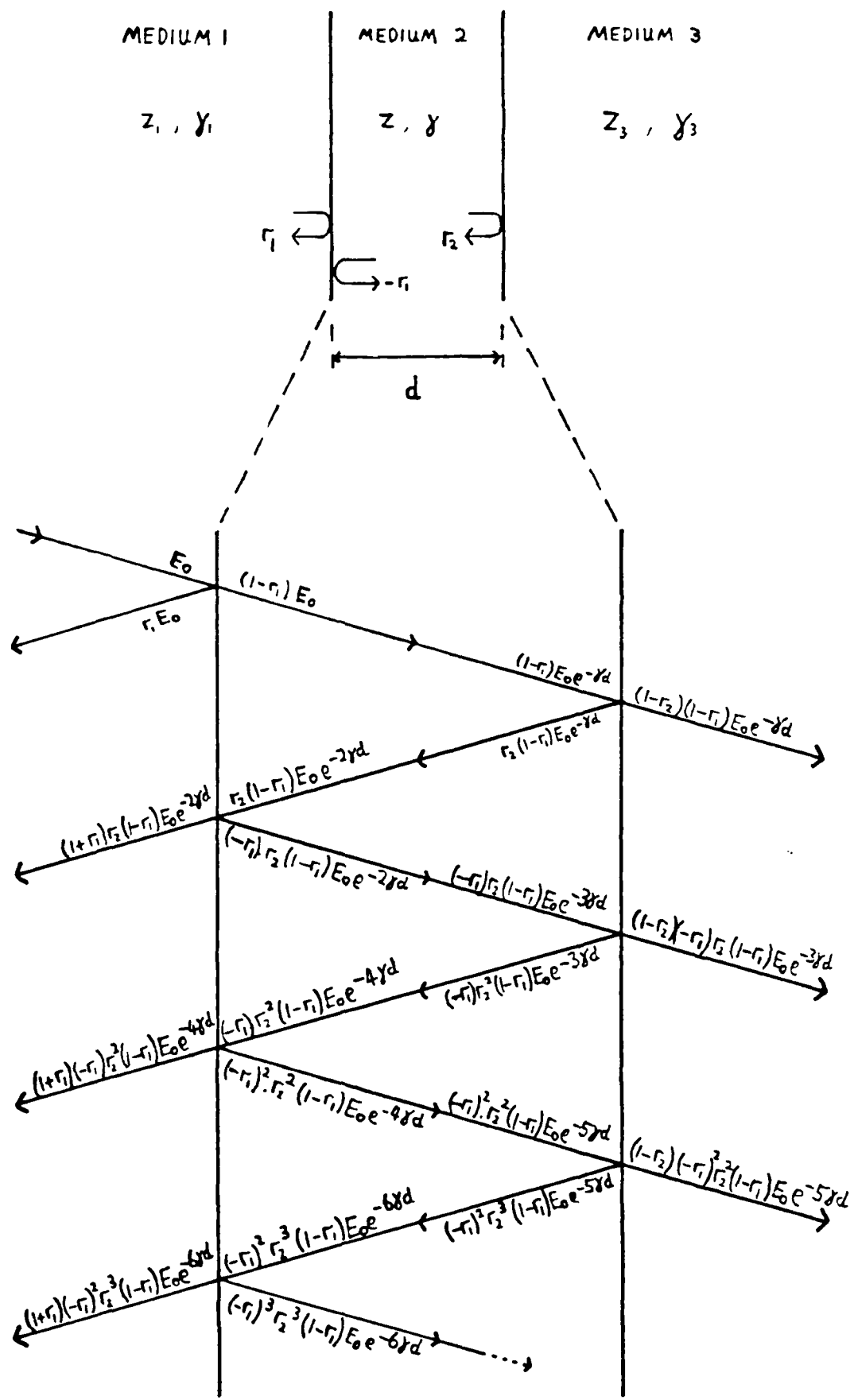
$(-r_1)^3 r_2^3(1-r_1)E_0 e^{-6\gamma d}$

Fig A3.1　The sequence of reflection/refraction events occurring within the finite layer of medium 2 when a wave is incident from medium 1. The phase and amplitude of each part wave is also indicated.

$$E_r = E_o r_1 + (1+r_1)(1-r_1)(r_2 \, e^{-2\gamma d} + (-r_1)r_2^2 \, e^{-4\gamma d} + (-r_1)^2 r_2^3 \, e^{-6\gamma d} +$$

$$+ \ldots) \qquad\qquad (A3.3)$$

Summing this and dividing by the incident wave, E_o, gives the reflection coefficient, Γ,

$$\Gamma = \frac{r_1 + r_2 \, e^{-2\gamma d}}{1 + r_1 r_2 \, e^{-2\gamma d}} \qquad . \qquad\qquad (A3.4)$$

Two specific cases can be considered immediately. If medium 3 is the same as medium 1, then $r_2 = -r_1$ and

$$\Gamma = \frac{r_1(1 - e^{-2\gamma d})}{1 - r_1^2 \, e^{-2\gamma d}} \qquad . \qquad\qquad (A3.5)$$

Alternatively, if medium 3 is a metal, $r_2 = -1$ and

$$\Gamma = \frac{r_1 - e^{-2\gamma d}}{1 - r_1 \, e^{-2\gamma d}} \qquad . \qquad\qquad (A3.6)$$

These equations express the reflection coefficient of the slab arrangement, Γ, in terms of the boundary reflection coefficients r_1 and r_2, and the exponential of the slab material's propagation factor, (γd). There are occasions when this formulation is more convenient than the alternative where Γ is expressed in terms of the intrinsic impedance of the slab, Z, and the hyperbolic tangent of (γd), which is obtained using equations (2.9) and (2.12).

A similar argument leads to the transmission coefficient, τ,

$$\tau = \frac{(1-r_2)(1-r_1) \, e^{-\gamma d}}{1 + r_1 r_2 \, e^{-2\gamma d}} \qquad\qquad (A3.7)$$

51

which, for the case when medium 3 and medium 1 are the same, reduces to

$$\tau = \frac{(1-r_1^2) \; e^{-\gamma d}}{1 - r_1^2 \; e^{-2\gamma d}} \qquad .$$

APPENDIX A4.   THE DECIBEL (dB) FOR EXPRESSING REFLECTIVITY

The decibel or dB scale is a logarithmic scale used to express ratios when wide dynamic ranges need to be expressed. The power ratio P_1/P_2 expressed in decibels, A, is given by

$$A = 10 \log_{10} \frac{P_1}{P_2} \text{ dB} \qquad (A4.1)$$

Some often used values are listed in the table:

$\frac{P_1}{P_2}$	100	10	2	1	$\frac{1}{2}$	$\frac{1}{10}$	$\frac{1}{100}$	$\frac{1}{1000}$
A (dB)	20	10	3	0	-3	-10	-20	-30

Thus, if the power output of a network is 10% of the power level at the input, the signal has incurred a power loss of, or been attenuated by, 10 dB - or alternatively, the network can be considered to have a power gain of -10 dB. In the case of microwave absorbers, an absorbent coating on a metal plate is said to have a reflection loss of 10 dB (sometimes written as -10 dB to emphasise that the return signal is reduced) if the reflected power is 10% of that reflected by the same plate without the coating.

Sometimes ratios of voltages or electric fields are used to represent power ratios. Because power is proportional to the square of the voltage, the power ratio in dB can be expressed as

$$A = 20 \log_{10} \frac{V_1}{V_2} \text{ dB} \qquad (A4.2)$$

The reflection coefficient, Γ, was defined in equation (2.10) as the ratio of the incident to reflected electric field, bu. the reflection loss, L_d, of a microwave absorber is expressed in terms of a power ratio. Therefore

$$L_d = 20 \log_{10} \left| \frac{1}{\Gamma} \right| \text{ dB} \qquad (A4.3)$$

53

Notice that the phase information inherent in Γ, which is a complex quantity, is lost when its magnitude only is taken in calculating reflection loss.

Overall security classification of sheet ....Unclassified..

(As far as possible this sheet should contain only unclassified information. If it is necessary to enter
classified information, the box concerned must be marked to indicate the classification eg (R) (C) or (S))

1. DRIC Reference (if known)	2. Originator's Reference Report No 85016	3. Agency Reference	4. Report Security U/C Classification
5. Originator's Code (if known)	6. Originator (Corporate Author) Name and Location Royal Signals and Radar Establishment		
5a. Sponsoring Agency's Code (if known)	6a. Sponsoring Agency (Contract Authority) Name and Location		

7. Title

An Introduction to Radar Absorbent Materials (RAM)

7a. Title in Foreign Language (in the case of translations)

7b. Presented at (for conference papers) Title, place and date of conference

8. Author 1 Surname, initials Lederer, P G	9(a) Author 2	9(b) Authors 3,4...	10. Date	pp. ref.
11. Contract Number	12. Period	13. Project	14. Other Reference	

15. Distribution statement

UNLIMITED

Descriptors (or keywords)

continue on separate piece of paper

Abstract

The purpose of this Introduction is to present, in a straightforward way,
the electromagnetic principles of Radar Absorbent Materials (RAM) for the
benefit of the non-electromagnetic-specialist who finds himself involved in this
field. The fundamental theory of electromagnetic wave propagation in media and
at the interfaces between different media is reviewed and the various approaches
to absorber design are described in the light of this. The types of materials
required and the techniques for measuring both their electromagnetic properties
and the performance of the finished absorber are outlined. Finally a means
of designing absorbers from a knowledge of the properties of its constituent
materials is described.

S80/48

END

DTIC

8-86